3-1-2019

Similarities and differences in circuit responses to applied Gly ^{1} -SIFamide and peptidergic (Gly ^{1} -SIFamide) neuron stimulation

Dawn M. Blitz
Miami University

Andrew E. Christie
Pacific Biosciences Research Center

Aaron P. Cook
University of Pennsylvania Perelman School of Medicine

Patsy S. Dickinson
Bowdoin College

Michael P. Nusbaum
University of Pennsylvania Perelman School of Medicine

Follow this and additional works at: https://digitalcommons.bowdoin.edu/biology-faculty-publications

Recommended Citation

RESEARCH ARTICLE | *Neural Circuits*

Similarities and differences in circuit responses to applied Gly^1-SIFamide and peptidergic (Gly^1-SIFamide) neuron stimulation

Dawn M. Blitz,[1]* **Andrew E. Christie,**[2]* **Aaron P. Cook,**[3]* **Patsy S. Dickinson,**[4] **and Michael P. Nusbaum**[3]

[1]*Department of Biology, Miami University, Oxford, Ohio;* [2]*Békésy Laboratory of Neurobiology, Pacific Biosciences Research Center, School of Ocean & Earth Science & Technology, University of Hawaii at Manoa, Honolulu, Hawaii;* [3]*Department of Neuroscience, Perelman School of Medicine, University of Pennsylvania, Philadelphia, Pennsylvania; and* [4]*Department of Biology, Bowdoin College, Brunswick, Maine*

Blitz DM, Christie AE, Cook AP, Dickinson PS, Nusbaum MP. Similarities and differences in circuit responses to applied Gly^1-SIFamide and peptidergic (Gly^1-SIFamide) neuron stimulation. *J Neurophysiol* 121: 950–972, 2019. First published January 16, 2019; doi:10.1152/jn.00567.2018.—Microcircuit modulation by peptides is well established, but the cellular/synaptic mechanisms whereby identified neurons with identified peptide transmitters modulate microcircuits remain unknown for most systems. Here, we describe the distribution of GYRKPPFNGSIFamide (Gly^1-SIFamide) immunoreactivity (Gly^1-SIFamide-IR) in the stomatogastric nervous system (STNS) of the crab *Cancer borealis* and the Gly^1-SIFamide actions on the two feeding-related circuits in the stomatogastric ganglion (STG). Gly^1-SIFamide-IR localized to somata in the paired commissural ganglia (CoGs), two axons in the nerves connecting each CoG with the STG, and the CoG and STG neuropil. We identified one Gly^1-SIFamide-IR projection neuron innervating the STG as the previously identified modulatory commissural neuron 5 (MCN5). Brief (~10 s) MCN5 stimulation excites some pyloric circuit neurons. We now find that bath applying Gly^1-SIFamide to the isolated STG also enhanced pyloric rhythm activity and activated an imperfectly coordinated gastric mill rhythm that included unusually prolonged bursts in two circuit neurons [inferior cardiac (IC), lateral posterior gastric (LPG)]. Furthermore, longer duration (>30 s) MCN5 stimulation activated a Gly^1-SIFamide-like gastric mill rhythm, including prolonged IC and LPG bursting. The prolonged LPG bursting decreased the coincidence of its activity with neurons to which it is electrically coupled. We also identified local circuit feedback onto the MCN5 axon terminals, which may contribute to some distinctions between the responses to MCN5 stimulation and Gly^1-SIFamide application. Thus, MCN5 adds to the few identified projection neurons that modulate a well-defined circuit at least partly via an identified neuropeptide transmitter and provides an opportunity to study peptide regulation of electrical coupled neurons in a functional context.

NEW & NOTEWORTHY Limited insight exists regarding how identified peptidergic neurons modulate microcircuits. We show that the modulatory projection neuron modulatory commissural neuron 5 (MCN5) is peptidergic, containing Gly^1-SIFamide. MCN5 and Gly^1-SIFamide elicit similar output from two well-defined motor circuits. Their distinct actions may result partly from circuit feedback onto the

MCN5 axon terminals. Their similar actions include eliciting divergent activity patterns in normally coactive, electrically coupled neurons, providing an opportunity to examine peptide modulation of electrically coupled neurons in a functional context.

central pattern generator; immunoreactivity; modulatory commissural neuron 5 (MCN5); stomatogastric ganglion (STG)

INTRODUCTION

Peptides represent the largest and most diverse class of neuronal signaling molecules used by animals (Christie et al. 2010; Merighi et al. 2011; Taghert and Nitabach 2012; van den Pol 2012). Neuropeptides can produce far-reaching hormonal actions and/or act relatively locally, often in parallel with small molecule transmitters, when released within a synaptic neuropil (Nusbaum et al. 2017). In most cases, the effects of peptides are modulatory, acting via metabotropic receptors. The resulting functional, circuit-level consequences of these modulatory actions have been examined in detail in several particularly accessible microcircuits (Jékely et al. 2018; Ko et al. 2015; Nässel 2002; Nusbaum et al. 2017; Nusbaum and Blitz 2012; Taghert and Nitabach 2012). A limitation of some of these studies, however, is that function was assessed using exogenous peptide application or manipulation of peptide receptor function in neuronal populations that are not necessarily all targets of a single peptidergic input. Despite the fact that neuronally released peptide often acts in a paracrine manner, its actions are not always well mimicked by the aforementioned approaches (Nusbaum et al. 2017). Yet there are only a small number of identified peptidergic neurons with elucidated circuit actions (e.g., Blitz et al. 1999; Wood et al. 2000; Chalasani et al. 2010; Kwiatkowski et al. 2013; Qiu et al. 2016; Clark et al. 2018; Cropper et al. 2018b).

Two well-defined microcircuits in which neuropeptide modulation has been extensively examined are the gastric mill (chewing) and pyloric (filtering of chewed food) circuits in the stomatogastric ganglion (STG), within the decapod crustacean stomatogastric nervous system (STNS) (Marder and Bucher 2007; Stein 2017). These circuits are flexible constructs that generate different versions of the gastric mill and pyloric

rhythms in response to different neuronal and hormonal modulatory actions, including the influence of many different neuropeptides (Dickinson et al. 2016; Marder 2012; Nusbaum et al. 2017; Stein 2009). This circuit flexibility may reflect the fact that many decapod crustaceans are highly opportunistic feeders, perhaps requiring numerous chewing and filtering patterns to accommodate a varied diet (Dickinson et al. 2008b; Donahue et al. 2009; Stehlik 1993).

Among the decapods, the chemical neuroanatomy of the crab *Cancer borealis* STNS is arguably the best elucidated (Chen et al. 2014; Marder 2012). Currently, over 200 candidate peptides have been identified from the *C. borealis* nervous system (Chen et al. 2014; Christie and Pascual 2016; Ma et al. 2009), many within the STNS and/or in the neuroendocrine organs that release peptide hormones to influence it. In parallel, the identity and actions of a few peptidergic projection neurons responsible for providing local modulation to the gastric mill and pyloric circuits are established (Nusbaum et al. 2001, 2017).

One neuropeptide identified previously by mass spectrometry and in silico transcriptome mining in the *C. borealis* STNS is a NH_2-terminally extended SIFamide peptide, GYRKP-PFNGSIFamide (Gly¹-SIFamide) (Chen et al. 2014; Christie and Pascual 2016; Huybrechts et al. 2003; Ma et al. 2009; Stemmler et al. 2007). The structural conservation of SIF-amides in arthropods is well established, and similar expression patterns occur in many insect species (Christie et al. 2006; Dickinson et al. 2008a; Polanska et al. 2007; Rehm et al. 2008; Verleyen et al. 2004; Yasuda et al. 2004; Yasuda-Kamatani and Yasuda 2006). Additionally, there is high sequence similarity between SIFamide receptors in the insect species in which they have been identified (Lismont et al. 2018). Although its cellular-level actions on the associated circuit neurons are yet to be elucidated in many cases, a role for SIF-amides has been identified in such diverse behaviors as sleep, aggression, and digestive functions as well as sexual and feeding behaviors (Martelli et al. 2017; Park et al. 2014; Sellami and Veenstra 2015; Terhzaz et al. 2007; Vázquez-Acevedo et al. 2009). In the STNS, SIFamides have only been examined in the lobster *Homarus americanus* (Christie et al. 2006; Dickinson et al. 2008a; Rehm et al. 2008). In this species, a Val¹ isoform is present and widely distributed in the STNS, and its bath application excites/modulates the pyloric rhythm (Christie et al. 2006; Dickinson et al. 2008a; Rehm et al. 2008).

Here, we established that Gly¹-SIFamide immunoreactivity (Gly¹-SIFamide-IR) is present in the *C. borealis* STNS, including the STG neuropil. Furthermore, applying this peptide to the isolated STG caused a concentration-dependent excitation of the pyloric rhythm and, at higher concentrations, also activated a gastric mill rhythm that included unusually prolonged bursting by two circuit neurons [inferior cardiac neuron (IC), lateral posterior gastric neuron (LPG)]. We also determined that one of the two Gly¹-SIFamide-IR neurons in each commissural ganglion (CoG) that innervate the STG is the previously identified projection neuron MCN5 (modulatory commissural neuron 5) (Norris et al. 1996). Brief (~10 s) MCN5 stimulation configures a unique pyloric rhythm, due to its excitatory and inhibitory actions on pyloric circuit neurons (Norris et al. 1996). We determined here that longer duration MCN5 stimulation elicits a Gly¹-SIFamide-like gastric mill rhythm, in-

cluding the aforementioned prolonged IC and LPG neuron bursting. This prolonged LPG bursting causes LPG activity to periodically diverge from that of its electrically coupled neurons, with which it typically displays strongly coincident activity. Thus, Gly¹-SIFamide is likely a peptide (co)transmitter of the identified modulatory projection neuron MCN5. The ability of MCN5 and Gly¹-SIFamide to cause a rhythmic separation of the activity of electrically coupled neurons promises to provide a tractable system for examining peptide modulation of electrically coupled neurons operating within a well-described microcircuit.

MATERIALS AND METHODS

Animals and Tissue Collection

Jonah crabs (*C. borealis*) were purchased from the Stonington Lobster Co-operative (Stonington, ME), Fresh Lobster Company (Gloucester, MA), and Ocean Resources (Sedgwick, ME). The crabs were maintained in flow-through natural seawater tanks at ambient ocean temperature (10–14°C) or artificial seawater tanks (10–12°C). Crabs were anesthetized by packing in ice for 30–60 min. The foregut was then removed, bisected along the ventral midline, and pinned flat (dorsal side up) onto a Sylgard 184 (Fisher Scientific, Hampton, NH)-lined dish containing chilled (4°C) physiological saline (composition in mM: 440 NaCl, 11 KCl, 13 $CaCl_2$, 26 $MgCl_2$, 10 HEPES; adjusted to pH 7.4 with NaOH -or- 440 NaCl, 11 KCl, 13 $CaCl_2$, 26 $MgCl_2$, 5 maleic acid, 10 Trizma base; pH 7.4–7.6). The STNS was subsequently dissected off the foregut via manual microdissection (Gutierrez and Grashow 2009; Saideman et al. 2007a).

Anatomy

Whole mount immunolabeling. For whole mount immunocytochemistry, tissues were fixed for 12–24 h at 4°C in a 4% paraformaldehyde solution (EM grade; Electron Microscopy Sciences; Hatfield, PA; catalog no. 15710) in 0.1 M sodium phosphate buffer (*P*). After fixation, tissues were rinsed repeatedly (5-times) at 1-h intervals at room temperature (18–20°C) in *P* containing 0.3% Triton-X 100 (*P-Triton*). They were then incubated for ~72 h at 4°C in rabbit polyclonal anti-Val¹-SIFamide antiserum (immunogen: synthetic Val¹-SIFamide conjugated to bovine serum albumin via glutaraldehyde) (Christie et al. 2006) diluted 1:500 in *P-Triton* containing 10% normal donkey serum (NDS; Jackson ImmunoResearch Laboratories, West Grove, PA; catalog no. 017-000-121). After incubation in primary antibody, tissues were rinsed five times at 1-h intervals, at room temperature, in *P-Triton* and then incubated for 12–24 h at 4°C in Alexa Fluor 488-conjugated donkey anti-rabbit IgG (Invitrogen, Carlsbad, CA; catalog no. A-21206) diluted 1:300 in *P-Triton* containing 10% NDS. After incubation in secondary antibody, tissues were rinsed five times at 1-h intervals, at room temperature, in *P-Triton*, after which they were mounted between a glass microscope slide and coverslip in Vectashield Mounting Medium (Vector Laboratories, Burlingame, CA; catalog no. H-1000). Incubation in secondary antibody and subsequent processing was conducted in the dark; slides were stored at 4°C in the dark until examined for labeling.

For double labeling, the anti-SIFamide primary antibody was paired with an antibody generated against substance P (immunogen: synthetic substance P conjugated to bovine serum albumin via 1-ethyl-3-[3-dimethylaminopropyl]carbodiimide; clone NC1/34 HL; Abcam, Cambridge, MA; catalog no. ab150349) (Cuello et al. 1979). This rat monoclonal anti-substance P antibody was added to the SIFamide antibody solution at a final concentration of 1:500. For visualization of the substance P antibody, a 1:300 dilution of Alexa Fluor 594-conjugated donkey anti-rat IgG (Invitrogen; catalog no. A-21209) was added to the secondary antibody solution.

Specificity controls. Because our study is the first to use the anti-Val[1]-SIFamide antibody on *Cancer* crab neural tissue, preadsorption controls were conducted to assess the likelihood that the immunolabeling obtained using this polyclonal antiserum in the crab STNS reflected the presence of Gly[1]-SIFamide. Specifically, the primary antibody was incubated for 2 h at room temperature with a 10^{-5} M concentration of Gly[1]-SIFamide (custom synthesized by GenScript, Piscataway, NJ), APSGFLGMRamide [*C. borealis* tachykinin-related peptide Ia (CabTRP Ia; custom synthesized by the Biotechnology Center, University of Wisconsin, Madison, WI) (Christie et al. 1997b)], or RYLPT (proctolin; Bachem AG, King of Prussia, PA; catalog no. H-6865) before its use for whole mount immunolabeling (see above).

The anti-substance P antibody employed in our study has been used extensively for mapping the distribution of the native tachykinin (CabTRP Ia) in neural and gut tissues of *C. borealis* (Blitz et al. 1995, 1999; Christie et al. 1997b, 1997a, 2007; Goldberg et al. 1988), and its specificity for this peptide in the STNS of this species is well documented (Christie et al. 1997b).

Neurobiotin nerve backfilling. For experiments involving nerve backfilling, the STNS was dissected as described above and then pinned in a Sylgard-lined Petri dish containing chilled (4°C) physiological saline. A petroleum jelly well was constructed around the stomatogastric nerve (*stn*) and the saline within the well replaced with distilled water. After several rinses with distilled water, the well was drained and refilled with a solution of 10% Neurobiotin Tracer (Vector Laboratories; catalog no. SP-1120) in distilled water, after which the *stn* was transected within the well. For backfills via the oesophageal nerve and inferior oesophageal nerve (*on/ion*), the paired superior oesophageal nerves (*son*s) were first transected to prevent the tracer from traveling to the CoGs via these nerves. Similarly, for backfills via the *son*, the *on* or the paired *ion*s were transected so that the sole route of tracer to the CoGs was via the *son*s. Preparations were then incubated at 4°C for ~48 h, with the saline surrounding the STNS replaced with fresh chilled saline after ~24 h. After the 48-h incubation, the CoGs were isolated, pinned in a new Sylgard-lined Petri dish, and then fixed and immunoprocessed for SIFamide and, in some cases, substance P labeling, as described above, with the exception that a 1:1,000 dilution of Alexa Fluor 594- (Invitrogen; catalog no. S-32356) or Alexa Fluor 647- (Invitrogen; catalog no. S-32357) conjugated streptavidin was added to the secondary antibody solution to allow visualization of the Neurobiotin-filled structures.

Imaging. Data were collected and digital images were generated using a Zeiss Axiovert 200 epifluorescence microscope (Carl Zeiss MicroImaging, Thornwood, NY) or an Olympus Fluoview 1000 confocal system (Olympus America, Center Valley, PA). The Axiovert 200 was equipped with EC Plan-NEOFLUAR ×10/0.3, LD Plan-NEOFLUAR ×20/0.4, and LD Plan-NEOFLUAR ×40/0.6 objective lenses (all dry), an EXFO X-Cite Series 120 halide arc lamp (EXFO Photonic Solutions, Mississauga, Ontario, Canada) and standard Zeiss FITC, Rhodamine and Cy5 filter sets. The Olympus Fluoview 1000 confocal system consisted of an Olympus IX-81 inverted microscope, ×10 Uplan S Apo, ×20 Uplan FLN, and ×40 Uplan S Apo objective lenses (all dry) and HeNe and multi-Ar lasers, as well as manufacturer-supplied Alexa Fluor 488, Alexa Fluor 594, and Alexa Fluor 647 filter sets and image-processing software.

For the production of figures, digital images were exported from the Olympus confocal system as .tiff files; composite figures were produced using CorelDraw (Corel, Ottawa, ON, Canada). The contrast and brightness of the final figures was adjusted to optimize the clarity of the printed images.

Electrophysiology

For electrophysiology experiments, the STNS, including all four ganglia plus their connecting and peripheral nerves, was dissected free from the foregut and pinned in a Sylgard-lined Petri dish (Gutierrez and Grashow 2009; Saideman et al. 2007a). The nervous system was continuously superfused (7–10 ml/min) with chilled (8–12°C) saline throughout experiments. Circuit neuron activity was monitored with intracellular recordings or with extracellular recordings from peripheral nerves. Extracellular recordings were accomplished with custom-made, paired stainless steel wire electrodes. One wire was placed alongside a nerve and isolated from the main bath compartment with petroleum jelly (Vaseline) and the other wire was placed in the bath, which also contained a common ground electrode. Recordings were amplified using model 1700 AC amplifiers (AM Systems, Carlsborg, WA).

Intracellular recordings were performed with borosilicate glass electrodes filled with 0.6 M K_2SO_4 plus 10 mM KCl or with 4 M potassium acetate (KAc) plus 10 mM KCl (20–25 MΩ) and connected to Axoclamp 2B or 900A amplifiers (Molecular Devices, San Jose, CA). MCN5 was recorded intrasomatically in the CoG (MCN5$_{CoG}$) or intra-axonally in the *stn*, within ~50 μm of the STG (MCN5$_{STG}$). To activate MCN5, current was injected using either bridge mode or discontinuous current clamp (5 kHz sampling rate). MCN5$_{CoG}$ was identified based on its axonal projection pattern and its previously described effects on pyloric circuit neurons (Norris et al. 1996). MCN5$_{STG}$ was identified based on the presence of its action potentials in an *ion* or in the simultaneously recorded MCN5 soma, and by intra-axonal depolarizing current injection causing the same response in pyloric circuit neurons as MCN5 soma stimulation (Norris et al. 1996) (Beenhakker MP, Norris BJ, Blitz DM, Nusbaum MP, unpublished observations). In some experiments, MCN5 was stimulated extracellularly in the *ion* (25–35 Hz tonic, 1-ms-duration pulses). MCN5 actions are distinct from those of MCN1, which is the only other CoG neuron to project to the STG via the *ion* (Bartos and Nusbaum 1997; Coleman et al. 1992; Coleman and Nusbaum 1994; Norris et al. 1996). To ensure that MCN1 would not have parallel actions in the STG when the *ion* was stimulated, we either photoinactivated MCN1$_{STG}$ or suppressed its cotransmitter release by loading it with acetate ions from a 4 M KAc-filled microelectrode (Coleman et al. 1995; Hooper and Marder 1987; Miller and Selverston 1979). MCN5 stimulation was performed using a Grass S88 stimulator and SIU5 stimulus isolation unit (Astro-Med/Grass Instruments, West Warwick, RI).

Pyloric- and gastric mill circuit neurons were identified based on the timing of their activity and the peripheral nerves in which their action potentials were recorded (Hooper et al. 1986; Marder and Bucher 2007). MCN1 action potentials were identified in extracellular *ion* recordings based on their pyloric- and gastric mill rhythm-timed activity pattern and persistent activation following stimulation of the dorsal posterior oesophageal nerve (*dpon*) (Beenhakker et al. 2004). Data were acquired in parallel onto chart recorder (AstroNova Everest Model, West Warwick, RI), and computer via a Micro 1401 data acquisition interface and Spike2 software (~5 kHz sampling rate) (Cambridge Electronic Design, Cambridge, UK).

Data Analysis

Data were analyzed primarily with Spike2 (Cambridge Electronic Design) software and Excel (Microsoft, Redmond, WA). Some MCN5 stimulation experiments predated the Spike2 system and were instead analyzed manually from chart recorder printouts. The pyloric rhythm response to Gly[1]-SIFamide application was analyzed only during times when the peptide did not also activate the gastric mill rhythm [e.g., no rhythmic bursting in the lateral gastric (LG) and dorsal gastric (DG) neurons, and no prolonged bursting by the IC neuron]. This was done because when both rhythms are active they influence one another (Bartos et al. 1999; Bartos and Nusbaum 1997; Blitz et al. 1999; Blitz and Nusbaum 2012).

Pyloric cycle period was analyzed by measuring the time between the onset of successive pyloric dilator (PD) neuron bursts (Bartos et al.

1999; Spencer and Blitz 2016). Burst duration was quantified as the duration from the first to the last action potential in a neuron burst. Phase relationships of pyloric neurons were determined by using PD as a reference for the beginning and end of each pyloric cycle. The phase of burst onset of other pyloric neurons was measured as the time from PD burst onset (i.e., pyloric cycle onset) to burst onset for each of the other neurons, divided by cycle period. Similarly, burst offset phase was measured as the time from PD burst onset to burst offset of each of the other pyloric neurons, divided by cycle period. The percent of a pyloric cycle during which a neuron was active (i.e., duty cycle) was calculated by dividing burst duration by cycle period. The gastric mill protraction phase is defined by LG neuron bursts, while the retraction phase is defined by the LG interburst period (Diehl et al. 2013; Heinzel et al. 1993; Spencer and Blitz 2016). Gastric mill cycle period was analyzed by measuring the time between the onset of successive LG bursts. In some experiments, ventricular dilator (VD) or DG activity was used to identify LG interbursts during MCN5 stimulation. VD is inhibited by LG and is thus only active during LG interbursts (Beenhakker et al. 2004; Spencer and Blitz 2016). In previously characterized gastric mill rhythms, DG alternates with LG (Beenhakker et al. 2004; Blitz et al. 2008; Coleman and Nusbaum 1994). DG burst period was quantified as the time from onset of a DG burst to the next DG burst, regardless of LG neuron activity.

For motor neurons that occur as a single copy [e.g., lateral pyloric (LP), IC, VD, LG, DG], the number of action potentials (i.e., spikes) per burst was quantified from extracellular recordings. For other neurons, which occur as multiple copies [PD 2, LPG 2, pyloric (PY) 3–5, gastric mill (GM) 4], the number of spikes/burst in each individual neuron could not be quantified from extracellular recordings because they contain the axons of most or all of a neuron type. Other activity parameters, such as burst duration and phase relationships, were quantified as population activity for a particular neuron type (e.g., 2 PD neurons). The one exception to measuring spike number from population activity was the measurement of LPG action potentials from extracellular recordings, which was done despite LPG occurring as a population of two neurons. Specifically, extension of LPG activity was quantified by counting the number of LPG action potentials that occurred after the end of a coincident PD neuron burst until the beginning of the next PD burst. Each spike waveform with a return to baseline between events was counted as an action potential, without distinguishing whether they represented an action potential in a single neuron, or a compound action potential from the two LPG neurons firing nearly synchronously. This approach likely underestimated the actual number of LPG spikes but nevertheless provided an effective comparison to controls, during which there were rarely any LPG spikes extending past the corresponding PD neuron burst. Unless otherwise indicated, data analysis was performed on 10 consecutive pyloric or gastric mill cycles. Notable exceptions are the analysis of pyloric cycle period vs. number of IC spikes per burst and the analysis of LPG burst extension compared with IC spike number. For these two analyses the number of cycles analyzed are reported in the RESULTS section.

Anatomical data are reported as mean ± standard deviation and electrophysiological data are reported as mean ± standard error. *N* values indicate number of preparations unless otherwise indicated. Neuronal activity parameters were statistically analyzed using ANOVA [repeated-measures (RM)-ANOVA, or Freidman RM-ANOVA on ranks] or Mann-Whitney rank sum test (SigmaPlot; Systat, San Jose, CA). Correlation analysis of IC burst duration and pyloric cycle period was performed using Pearson correlation (SigmaPlot) and least squares to fit the data from each experiment to a piecewise linear model: $y = m1 * x + b1$ for $x \leq$ theta or $y = m2 * x + b2$ for $x >$ theta, where theta $= (b2 - b1)/(m1 - m2)$, and $m1 \neq m2$. Reported *P*-values for this correlation analysis were based on an F-test comparing the piecewise fit to a null model that was a single, straight line (MATLAB; MathWorks, Natick, MA). For all statistical analysis, significance was considered to be $P < 0.05$.

RESULTS

SIFamide-Like Immunolabeling in the Crab STNS

The native SIFamide in *C. borealis* is GYRKPPFNGSIFamide (Gly^1-SIFamide). We previously developed an antibody to Val^1-SIFamide that cross-reacts with both the Val^1- and Gly^1-isoforms (Christie et al. 2006). Using this antibody, the distribution of Gly^1-SIFamide-IR was mapped in the STNS of *C. borealis*. The STNS is composed of four ganglia plus their connecting and peripheral nerves (Fig. 1). The ganglia include the paired CoGs (~500 neurons each), the unpaired oesophageal ganglion (OG: ~14 neurons), and the STG (~26 neurons) (Coleman et al. 1992; Follmann et al. 2017; Kilman and Marder 1996; Marder and Bucher 2007; Wiersma 1957). In *C. borealis*, there are approximately 20 pairs of CoG and OG neurons that project to the STG and influence the circuits therein (Coleman et al. 1992).

SIF-IR was present throughout the STNS (Fig. 2) (*n* = 12). Within each CoG, Gly^1-SIFamide-IR was present in ~20 somata [21.0 (SD 2.1); *n* = 12] and throughout the neuropil (Fig. 2*A*). All somatic immunolabeling was cytoplasmic and distinctly punctate in appearance. Most of the labeled somata were located near the insertions of the inferior oesophageal- (*ion*) and superior oesophageal (*son*) nerves (Fig. 2) and were relatively close to the dorsal surface of the ganglion (i.e., located just under the ganglionic sheath). Neuropil labeling in the CoG consisted of small immunopositive varicosities that studded fine neurites. The neuron(s) responsible for the neuropil labeling remains unknown. However, it is likely that some of the intrinsic Gly^1-SIFamide-IR CoG somata contribute to this labeling, as may Gly^1-SIFamide-IR axons projecting to the CoG via the circumoesophageal connectives (*cocs*), presumably from somata present in the brain and/or fused thoracic ganglion, neither of which was investigated in this study.

There was a single Gly^1-SIFamide-IR axon projecting through each *ion* and *son* from each CoG (*n* = 12). The immunolabeled *ion* axon projected through the oesophageal ganglion (OG) and oesophageal nerve (*on*) to its junction with the *sons* and the stomatogastric nerve (*stn*). At the anterior end of the *stn*, near its junction with the *on* and *sons*, an extensive neuropil region is present, which was replete with Gly^1-SIFamide-IR (Fig. 2*B*). The labeling in this region prevented the unambiguous tracking of the Gly^1-SIFamide-IR axon projection pathway further, though in a few preparations (*n* = 3/12) it appeared that the axon present in each *ion* entered the *stn*, projecting to and innervating the STG neuropil. Similarly, each *son*-projecting Gly^1-SIFamide-IR axon could be followed to the junction of the *on*, *son*, and *stn*, but there too the presence of the Gly^1-SIFamide-IR neuropil in the anterior *stn* prevented unambiguous determination of the axon projection pathway. Again, though, in several preparations (*n* = 4/12), each axon appeared to project to and innervate the STG neuropil. Additionally, four *stn* axons consistently exhibited Gly^1-SIFamide-IR near the entrance to the STG (*n* = 12) (Fig. 2*C*), a site posterior to the aforementioned *stn* neuropil.

Within the STG, Gly^1-SIFamide-IR was limited to fine neuropilar processes (*n* = 12) (Fig. 2*C*). This labeling derived entirely from the Gly^1-SIFamide-IR labeled *stn* axons. The Gly^1-SIFamide-IR varicosities were peripherally located within the STG neuropil, forming a rind around the central core of the neuropil, a distribution that has been noted for other
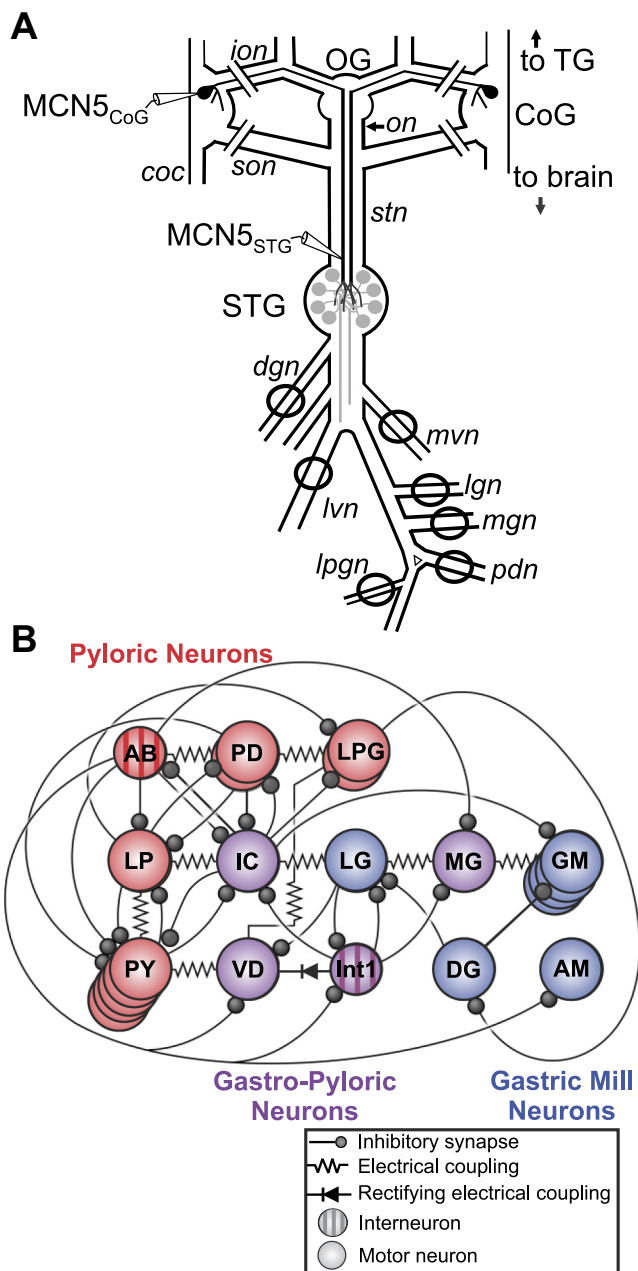
Fig. 1. Schematic representation of the stomatogastric nervous system in the crab *Cancer borealis*. *A*: schematic of the stomatogastric nervous system, including the projection pathway of the bilaterally paired projection neuron MCN5. Electrodes indicate recording locations from the MCN5 soma in the CoG (MCN5$_{CoG}$) or its axon near the entrance to the STG (MCN5$_{STG}$). Circles on nerves indicate recording sites for traces shown in later figures. Breaks in inferior and superior oesophageal nerves (*ion*, *son*) indicate where nerves were bisected for bath-application experiments. *B*: schematic of the gastric mill and pyloric circuits in *C. borealis*. There are eight gastric mill circuit neuron types, one of which is present as four apparently equivalent copies (GM neurons). This includes seven motor neurons and a single interneuron (Int1). There are seven pyloric circuit neuron types, including six motor neurons and one interneuron (AB). Three of these neuron types are present as multiple, apparently equivalent copies (PD: 2; LPG: 2; PY: 5). These neurons exhibit pyloric rhythm-timed activity (red), gastric mill rhythm-timed activity (blue), or a combination of pyloric- and gastric mill rhythm-timed activity (purple). Both panels are modified, with permission, from Nusbaum et al. (2017).

modulator labeling (Christie et al. 1997a). No Gly¹-SIF-amide-IR somata were evident in the STG ($n = 12$), nor was any labeling consistently present in the peripheral nerves of the STG ($n = 11/12$). Lastly, within the OG, the only Gly¹-SIFamide-IR present was that within the labeled axons projecting from each *ion* through the OG to the *on* ($n = 12$).

Specificity Controls

To confirm that the immunostaining reported above was the result of the Val¹-SIFamide antibody binding to Gly¹-SIF-amide, we conducted preadsorption controls in which the SIFamide antibody was preincubated with Gly¹-SIFamide, CabTRP Ia, or proctolin (in each case: 10^{-5} M) before its application to the tissue. Preadsorption of the antibody with Gly¹-SIFamide abolished all labeling in the STNS ($n = 3$), while preadsorption with CabTRP Ia or proctolin did not affect Gly¹-SIFamide-IR ($n = 3$ preparations per peptide).

Neurobiotin Nerve Backfill and Gly¹-SIFamide-IR Double-Labeling in the C. borealis STNS

In *C. borealis*, most modulatory innervation to the STG originates from ~20 projection neurons in each CoG (Coleman et al. 1992). To determine whether the somata responsible for the Gly¹-SIFamide-IR in the *C. borealis* STG were among those CoG neurons, we performed Neurobiotin tracer backfilling of the *stn* to the CoGs, either via the *son*s (with *ion*s bisected) or via the *on* and *ion*s (with *son*s bisected). These backfilled CoGs were subsequently immuno-processed for Gly¹-SIFamide-IR. In agreement with the previous study (Coleman et al. 1992), Neurobiotin visualization with streptavidin (see MATERIALS AND METHODS) revealed ~20 labeled somata in each CoG [19.8 (SD 0.8); $n = 10$] when backfilling via the *son*s, and ~2 filled somata [20 (SD 0.3); $n = 15$ preparations] when backfilling via the *on/ion*s. On average, there was 1 soma in each CoG that was double labeled with Neurobiotin and Gly¹-SIFamide-IR when the *son* was backfilled [1.0 (SD 0.3); $n = 10$], and another 1 soma [0.9 (SD 0.2); $n = 15$] in each CoG when the *on/ion* was backfilled (Fig. 3). It thus appears that all Gly¹-SIFamide-IR in the STG originates from four CoG somata, including one per ganglion projecting to the STG via the *son* and one projecting via the *ion* and *on*.

Gly¹-SIFamide-IR in MCN5

Of the ~20 CoG somata projecting to the STG, only two of them do so via the *ion* and *on* (Coleman et al. 1992). The axons of the remaining CoG projection neurons travel through the *son* to innervate the STG. Both projection neurons that project through the *ion/on* are identified and characterized physiologically. These neurons are modulatory commissural neurons 1 and 5 (MCN1, MCN5) (Coleman and Nusbaum 1994; Norris et al. 1996). MCN1 has three known cotransmitters, including GABA and the peptides proctolin and CabTRP Ia (Blitz et al. 1999; Nusbaum et al. 2017). Other projection neurons innervating the *C. borealis* STG also contain GABA and/or proctolin (Blitz et al. 1999; Nusbaum et al. 2017; Nusbaum and Marder 1989a). However, MCN1 is the sole source of CabTRP Ia innervation to the *C. borealis* STG and is the only source of the CabTRP-IR axons in the *ion*s, *on* and *stn* (Blitz et al. 1995, 1999; Christie et al. 1997b; Goldberg et al. 1988). In contrast,
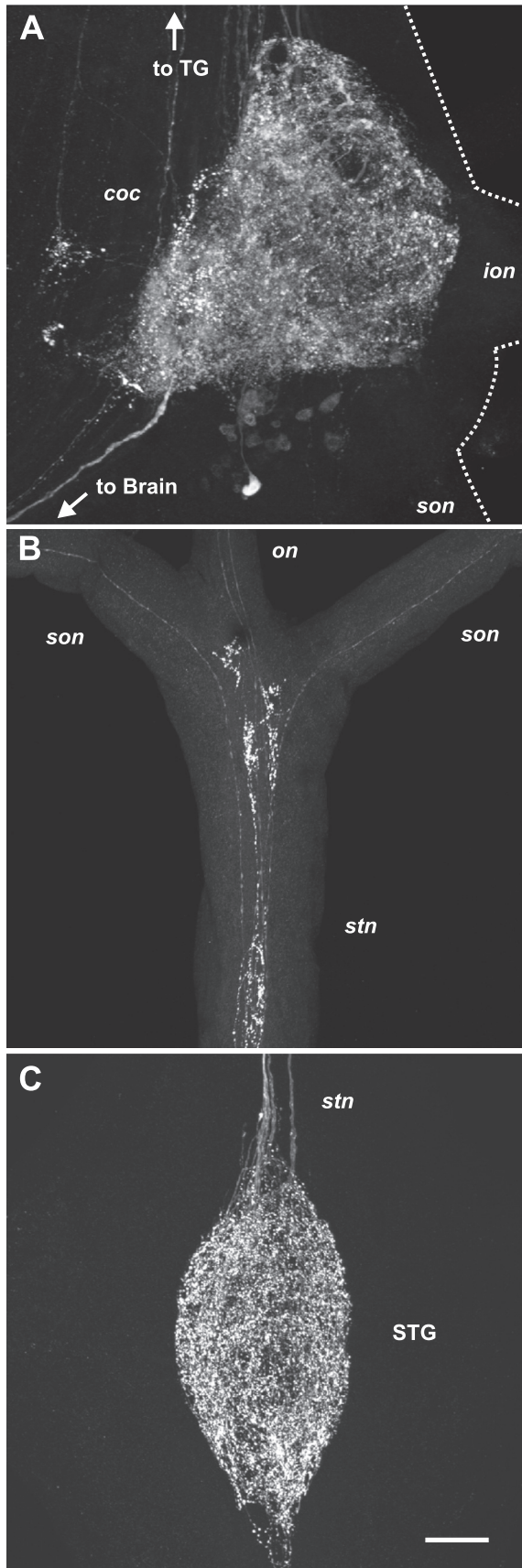
the MCN5 (co)transmitter phenotype remains unknown (Norris et al. 1996).

To determine whether the SIFamide-IR axon projecting through the *ion* was that of MCN1 or MCN5, we examined preparations double-IR labeled for colocalization of Gly[1]-SIFamide and CabTRP Ia in the *stn* axons (Fig. 4*A*) and in the STG neuropil (data not shown). We found no Gly[1]-SIFamide- and CabTRP-IR colocalization in *stn* axons ($n = 7$), indicating that the CoG Gly[1]-SIFamide-IR somata that project to the STG via the *ion/on* pathway are the paired MCN5s, and not the paired MCN1s. To confirm the identity of the Gly[1]-SIF-amide-IR CoG neuron projecting an axon through the *ion* and *stn* to the STG, we combined Neurobiotin backfills of the *stn* (with the *son*s transected) with Gly[1]-SIFamide-IR and CabTRP-IR (see MATERIALS AND METHODS). As shown in Fig. 4*B*, under these conditions, one of the two somata backfilled through the *ion* exhibited Gly[1]-SIFamide-IR, while the other backfilled soma exhibited CabTRP-IR ($n = 4$). Thus, the Gly[1]-SIFamide-IR CoG soma projecting to the STG via the *ion* and *on* is the identified projection neuron MCN5.

Gly[1]-SIFamide Excites the C. borealis STG Motor Patterns

The STG circuits generate the pyloric and gastric mill rhythms. The pyloric rhythm is continuously active in vivo and in vitro, due largely to the continuous modulatory influences it receives from projection neurons and circulating hormones (Marder and Bucher 2007; Stein 2017). The gastric mill rhythm is instead episodic, both in vivo and in vitro, as its activation is driven by CoG projection neurons which themselves are not spontaneously active (Beenhakker and Nusbaum 2004; Blitz et al. 2004, 2008; Christie et al. 2004; Diehl et al. 2013). We assessed responses of the pyloric and gastric mill rhythms to Gly[1]-SIFamide application with CoG projection neuron inputs removed by bisecting the *ion*s and *son*s (Fig. 1). In such preparations, with the *C. borealis* STG superfused with saline (8–12°C), the pyloric rhythm slows or terminates and the gastric mill rhythm terminates if it was active (Bartos and Nusbaum 1997; Hamood et al. 2015; Hamood and Marder 2014).

Effects of Gly[1]-SIFamide on the Pyloric Rhythm

The *C. borealis* pyloric rhythm is a three-phase motor pattern that generates the pumping and filtering actions that move chewed food from the foregut to the midgut (Marder and Bucher 2007). This rhythm is driven by a group of electrically coupled pacemaker neurons that includes a conditional burster interneuron, anterior burster (AB), plus the paired PD and LPG motor neurons. Overall, the pyloric circuit contains seven

Fig. 2. Gly[1]-SIFamide immunoreactivity in the stomatogastric nervous system of *C. borealis*. *A*: SIFamide immunolabeling in the CoG. In addition to immunolabel throughout the neuropil, ~20 cell bodies were consistently and clearly labeled in each CoG. *B*: SIFamide immunolabeling occurred in four axons near the *son/stn* junction, including one that projected from each of the two *ion*s and then through the oesophageal nerve (*on*), and one that projected from each of the two *son*s. No cell bodies were labeled at the *son/stn* junction, but additional neuropil was immunolabeled. All four axons projected past the neuropil label in the *stn* toward the STG. *C*: SIFamide immunolabeling in the STG was extensive, all of which originated from the two pairs of *stn* axons. No STG cell bodies, all of which are present surrounding the neuropil, were immunolabeled. Scale bar in *C* = 100 μm and applies to all panels.
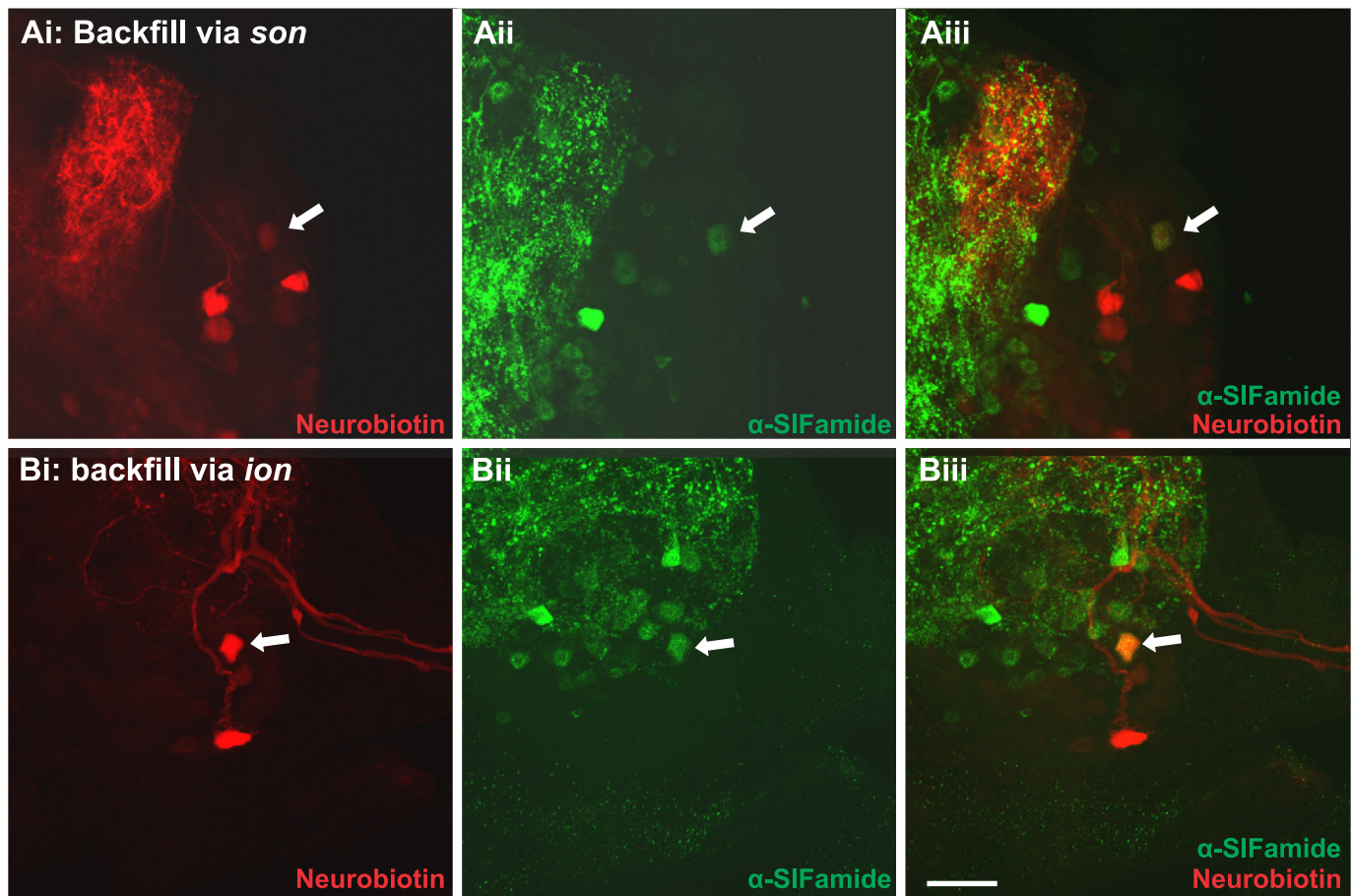
Fig. 3. Gly[1]-SIFamide-immunoreactivity in the STG is derived from two neurons in each CoG. *Ai*: Neurobiotin labeling as a result of a *stn* backfill, after bisecting the *ion* nerves, reveals multiple CoG cell bodies as well as extensive neuropil labeling. These labeled somata have axons projecting to the STG via the *son* and *stn*, or are dye-coupled to neurons that do so. *Aii*: More extensive Gly[1]-SIFamide-IR labeling in the CoG neuropil and a larger number of immunolabeled somata are evident. *Aiii*: overlap of Gly[1]-SIFamide-IR and Neurobiotin labeling identifies a single double-labeled SIFamide-containing soma that projects through the *son* and *stn* to the STG. All three panels are the same field of view in the same CoG. Arrows in *A*, *i–iii* point to the same cell body in each image. *Bi*: Neurobiotin labeling in a CoG resulting from a *stn* backfill after the *son* nerves were bisected identifies two somata with axons projecting through the *ion* and *stn* to the STG. *Bii*: Gly[1]-SIFamide-IR is again expressed extensively in the CoG neuropil and multiple somata. *Biii*: an overlay of Gly[1]-SIFamide-IR and Neurobiotin labeling in the CoG reveals a single double-labeled SIFamide-containing neuron that projects an axon through the *ion* and *stn* to the STG. All three panels are the same field of view in the same CoG. Arrows in *B*, *i–iii* point to the same neuronal cell body. Scale bar in *Biii* = 100 μm and applies to all panels.

neuron types, including the aforementioned pacemaker group (Fig. 1*B*) (Nusbaum et al. 2017). The canonical pyloric rhythm cycle is designated to begin with a burst of spikes in the pacemaker group, followed after a pause by activity in the LP and IC neurons, after which the PY and VD neurons are active (Fig. 5) (Hamood et al. 2015; Nusbaum et al. 2017). Some pyloric neurons (e.g., IC, VD) also exhibit a gastric mill rhythm-associated burst pattern (see *Effects of Gly[1]-SIFamide on the Gastric Mill Rhythm*) (Nusbaum et al. 2017).

Superfusing Gly[1]-SIFamide onto the STG had concentration-dependent effects on the pyloric rhythm (Fig. 5, Tables 1, 2, and 3). When the pyloric rhythm persisted during saline superfusion in the isolated STG, the Gly[1]-SIFamide threshold concentration for altering this rhythm was $>10^{-9}$ M. For example, whereas none of the analyzed pyloric rhythm parameters were altered by the presence of 10^{-9} M Gly[1]-SIFamide ($n = 6$), at 10^{-8} M Gly[1]-SIFamide ($n = 11$) the pyloric cycle period decreased by ~20% and the PD neuron burst duration decreased by ~14%, resulting in the PD neuron duty cycle (i.e., percentage of a normalized cycle when a neuron is active) increasing by ~10% (Fig. 5, Table 1). The number of IC neuron

action potentials per pyloric burst also increased, albeit with considerable variability across preparations (Fig. 5). As presented below, IC activity was further altered during Gly[1]-SIFamide bath applications in which a gastric mill rhythm was activated. In the two preparations in which there was no regular pyloric rhythm after isolation, the rhythm was reactivated by 10^{-9} M Gly[1]-SIFamide application (data not shown).

Some pyloric rhythm parameters that were not altered at the threshold concentration were changed, in the same experiments, when higher Gly[1]-SIFamide concentrations were applied. For example, the threshold response was 10^{-7} M Gly[1]-SIFamide for changes in the PD neuron burst termination phase (delayed ~14%), the number of spikes/burst in the LP neuron (increased ~28%), and the burst onset phase of the PY neurons (delayed ~15%) (Fig. 5; Tables 1, 2, and 3). One circuit neuron whose pyloric rhythm-timed activity was not consistently affected by Gly[1]-SIFamide application at any concentration was the VD neuron. As is common when the CoGs are removed, VD was silent during saline superfusion ($n = 59$). VD remained silent in most experiments even when relatively high Gly[1]-SIFamide con-
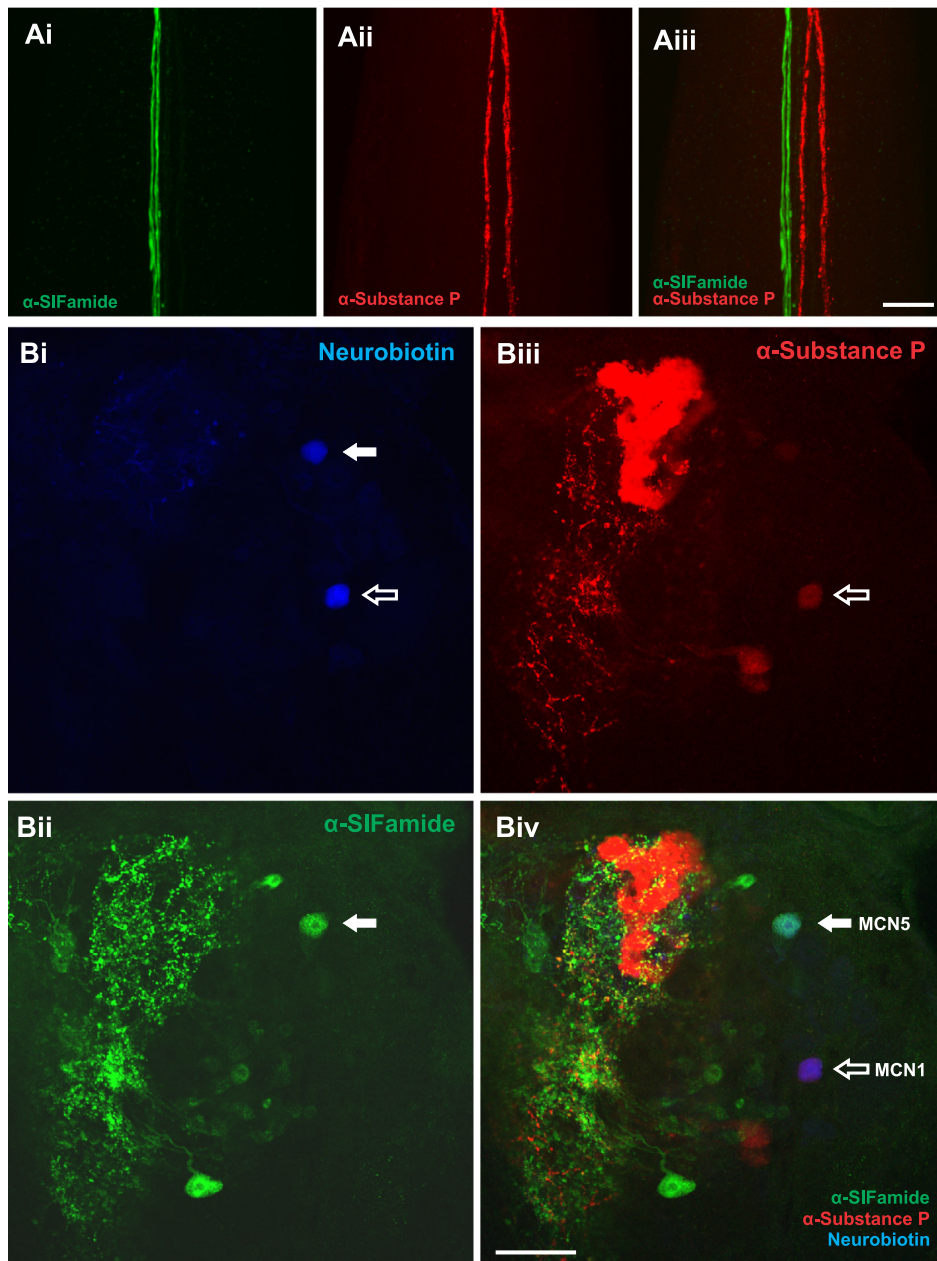
Fig. 4. One of the Gly[1]-SIFamide-IR neurons projecting from the CoGs to the STG is the identified projection neuron MCN5. *Ai*: Gly[1]-SIFamide-IR in the *stn* is limited to two pairs of closely bound axons which project between the anterior ganglia (CoGs and OG) and the STG. *Aii*: CabTRP Ia immunolabeling (α-substance P) in the *stn* labels two axons, shown previously to be the axons of the paired CoG projection neuron MCN1 (modulatory commissural neuron 1; Blitz et al. 1999). *Aiii*: a composite of the Gly[1]-SIFamide-IR and substance P-IR shows that these two labels are in distinct axons. As MCN5 and MCN1 are the only neurons that travel through the *ion*, these observations strongly suggest that the Gly[1]-SIFamide-IR CoG neuron that projects through the *ion* and *stn* is MCN5. Scale bar in *Aiii* = 25 μm and applies to *A*, *i–iii*. *Bi*: a Neurobiotin backfill of the *stn* with the *ion*s intact and *son*s bisected labeled two neurons. The same preparation was subsequently labeled with antibodies against Gly[1]-SIFamide (*Bii*) and substance P (*Biii*). *Biv*: an overlay of the Neurobiotin labeling with Gly[1]-SIFamide-IR and substance P-IR demonstrates that one Neurobiotin labeled neuron colabels with α-SIFamide and the other colabels with α-substance P. The unfilled arrow points to the same neuron in all images, identified as MCN1 (Blitz et al. 1999; Christie et al. 1997b; Coleman and Nusbaum 1994). The filled arrow points to the same neuron in all images, identified as MCN5 (Norris et al. 1996). Scale bar in *Biv* = 100 μm and applies to *Bi–iv*.

centrations were applied, unless the gastric mill rhythm was activated (VD unresponsive to Gly[1]-SIFamide: 10^{-7} M: $n = 7/10$; 10^{-6} M: $n = 3/6$) (see *Effects of Gly[1]-SIFamide on the Gastric Mill Rhythm*). Furthermore, in two of the three experiments in which only the pyloric rhythm was active during 10^{-6} M Gly[1]-SIFamide application, VD fired on average <1 spike/pyloric cycle. All of the Gly[1]-SIFamide actions on the pyloric rhythm persisted for the duration of bath applications (15–30 min) ($n = 14$).

Effects of Gly[1]-SIFamide on the Gastric Mill Rhythm

The gastric mill rhythm is a two-phase, episodic motor pattern that drives the chewing movements of the teeth within the gastric mill stomach compartment (Diehl et al. 2013; Heinzel 1988; Heinzel et al. 1993). Unlike the pyloric rhythm, which is activated by application of many different neuromodulators in the isolated *C. borealis* STG, the peptide CabPK (*C. borealis* pyrokinin; 10^{-6} M) is the only neuromodulator previously shown to activate the gastric mill rhythm when bath applied (Marder 2012; Rodriguez et al. 2013; Saideman et al. 2007b, 2007a). There is no amino acid sequence similarity between CabPK (Saideman et al. 2007b) and Gly[1]-SIFamide.

The gastric mill rhythm includes activity in eight neuron types, including seven motor neurons and one interneuron (Fig. 1*B*). The phases of the gastric mill rhythm refer to protraction and retraction of the teeth, with half of the circuit neurons primarily or exclusively active during the protraction phase, and the other half active during retraction (Nusbaum et al. 2017). The motor neurons are further subdivided into the lateral and medial tooth subsystems, primarily controlling the rhythmic protraction and retraction of the paired lateral teeth
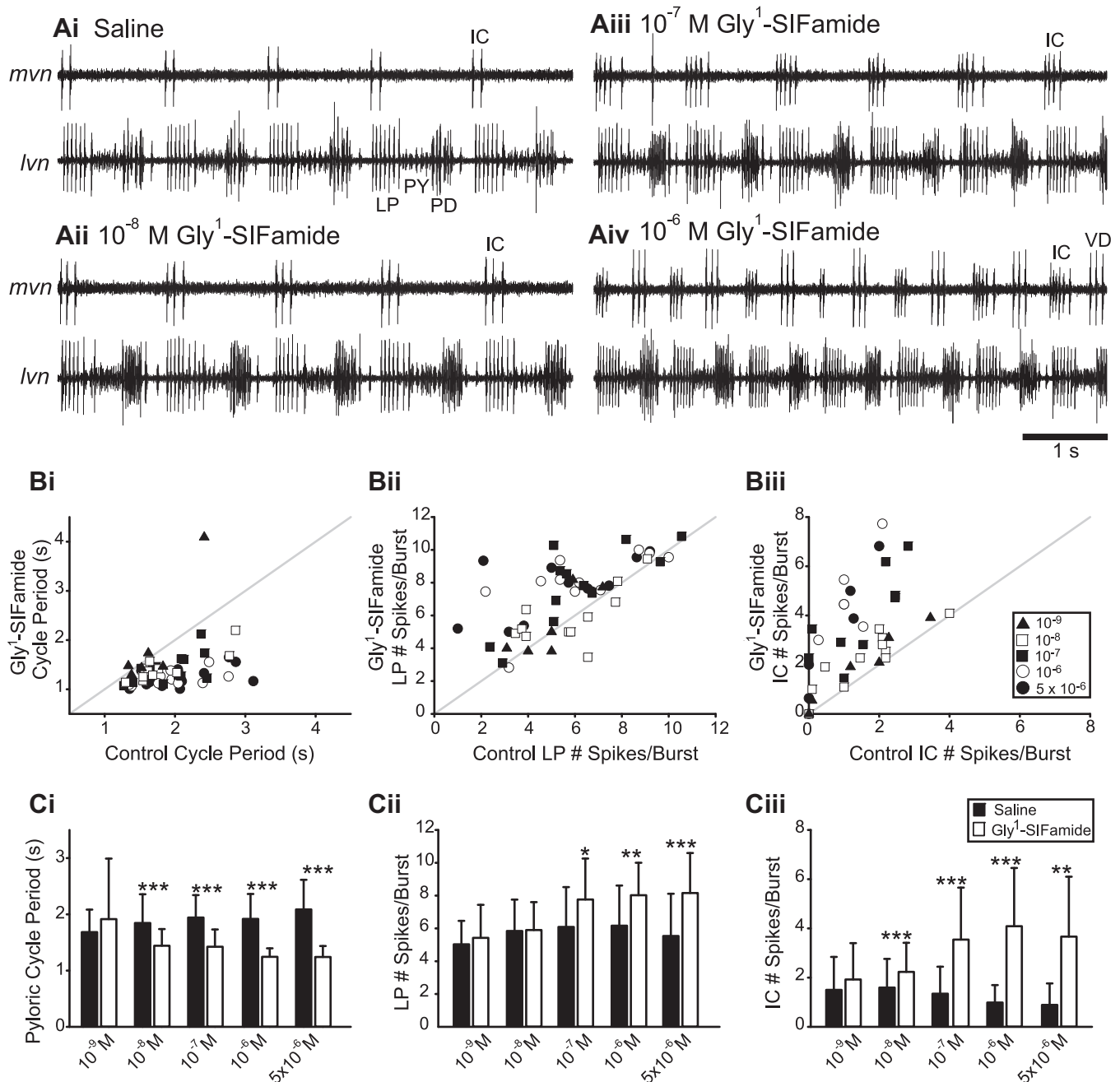
Fig. 5. Gly[1]-SIFamide produces a dose-dependent modulation of the pyloric rhythm in the isolated *C. borealis* stomatogastric ganglion (STG). *Ai*: during control saline superfusion, the pyloric circuit was active as evident in the rhythmic bursting activity of the four labeled pyloric neurons in the extracellular nerve recordings (*lvn*, *mvn*). *A*, *ii–iv*: Bath application of Gly[1]-SIFamide (10^{-8} to 10^{-6} M) had dose-dependent effects on the pyloric rhythm. For example, IC activity was increased at 10^{-8} M Gly[1]-SIFamide (*Aii*), but a change in LP neuron activity did not occur until 10^{-7} M Gly[1]-SIFamide (*Aiii*) and regular VD neuron bursting did not occur until 10^{-6} M Gly[1]-SIFamide (*Aiv*). All recordings are from the same preparation with a saline wash between applications. *B*: scatter plots of the pyloric cycle period (Bi), number of LP spikes per burst (*Bii*) and number of IC spikes per burst (*Biii*) in Gly[1]-SIFamide (10^{-9} to 5×10^{-6} M, see legend), plotted against their control values from multiple preparations. Each symbol indicates the average across multiple sequential pyloric cycles for one peptide application in one preparation. *C*: average ($\pm$SE) pyloric cycle period (*Ci*), number of LP spikes per burst (*Cii*), and number of IC spikes per burst (*Ciii*) in saline (black bars) and Gly[1]-SIFamide (white bars; 10^{-9} to 5×10^{-6} M) are plotted ($n = 5$–14). One way RM-ANOVA, Holm-Sidak post hoc; $*P < 0.05$; $**P < 0.01$; $***P < 0.001$.

(protraction: LG, MG, IC neurons; retraction: LPG, VD neurons) and unpaired medial tooth (protraction: GM neurons; retraction: DG neuron) (Heinzel et al. 1993). For the previously characterized gastric mill rhythm driven by the projection neuron MCN1, the rhythm generator includes the reciprocally inhibitory LG protractor motor neuron and interneuron 1

(Int1), which is active during retraction (Coleman et al. 1995; Nusbaum et al. 2017).

Bath application of relatively high Gly[1]-SIFamide concentrations to the isolated STG not only excited the pyloric rhythm but often activated a gastric mill rhythm that primarily involved the lateral tooth subsystem (10^{-6} M: $n = 6/14$; $5 \times$

Table 1. *Concentration-dependent modulation of PD neuron activity by Gly^1-SIFamide*

PD Parameter	Mean ± SE			F	df	P			n
	Pre	Peptide	Post			Pre vs. Peptide	Post vs. Peptide	Pre vs. Post	
Burst duration, s									
5×10^{-6}	0.35 ± 0.03	0.26 ± 0.02	0.34 ± 0.02	13.185*	13,2	**<0.001**	**<0.001**	0.698	14
10^{-6}	0.34 ± 0.03	0.27 ± 0.02	0.37 ± 0.03	23.187*	11,2	**<0.001**	**<0.001**	0.056	12
10^{-7}	0.37 ± 0.03	0.32 ± 0.03	0.40 ± 0.03	12.811*	11,2	**0.003**	**<0.001**	0.197	12
10^{-8}	0.34 ± 0.03	0.29 ± 0.02	0.34 ± 0.03	6.076*	10,2	**0.017**	**0.016**	0.829	11
10^{-9}	0.30 ± 0.01	0.31 ± 0.04	0.34 ± 0.03	1.738*	5,2		0.23		6
Phase off, % of pyloric cycle									
5×10^{-6}	16.7 ± 1.2	20.4 ± 0.7	16.9 ± 0.9	10.696*	13,2	**0.001**	**0.001**	0.878	14
10^{-6}	18.1 ± 1.3	21.8 ± 1.1	19.8 ± 1.5	7.887*	11,2	**0.002**	0.081	0.086	12
10^{-7}	19.2 ± 0.5	22.0 ± 1.0	19.5 ± 1.0	7.462*	11,2	**0.005**	**0.010**	0.659	12
10^{-8}	18.7 ± 1.4	20.0 ± 1.1	19.5 ± 1.2	1.575*	10,2		0.23		11
10^{-9}	18.0 ± 1.1	17.4 ± 1.6	18.4 ± 1.9	0.524*	5,2		0.61		6
Cycle period, s									
5×10^{-6}	2.09 ± 0.1	1.24 ± 0.05	2.04 ± 0.1	40.378*	13,2	**<0.001**	**<0.001**	0.642	14
10^{-6}	1.92 ± 0.1	1.24 ± 0.04	1.95 ± 0.2	24.650*	11,2	**<0.001**	**<0.001**	0.799	12
10^{-7}	1.94 ± 0.1	1.42 ± 0.09	2.05 ± 0.2	19.723*	11,2	**<0.001**	**<0.001**	0.352	12
10^{-8}	1.85 ± 0.2	1.44 ± 0.09	1.76 ± 0.1	13.630*	10,2	**<0.001**	**0.002**	0.325	11
10^{-9}	1.69 ± 0.2	1.92 ± 0.44	1.82 ± 0.5	0.33*	5,2		0.73		6
Duty cycle, % of pyloric cycle									
5×10^{-6}	16.9 ± 1.2	20.4 ± 0.6	16.9 ± 0.8	9.183*	13,2	**0.003**	**0.002**	0.923	14
10^{-6}	18.0 ± 1.2	21.4 ± 1.1	19.8 ± 1.5	6.948*	11,2	**0.004**	0.094	0.188	12
10^{-7}	19.2 ± 0.5	22.0 ± 1.0	19.5 ± 0.9	7.915*	11,2	**0.005**	**0.007**	0.715	12
10^{-8}	18.7 ± 1.4	20.1 ± 1.1	19.5 ± 1.1	1.764*	10,2		0.197		11
10^{-9}	18.1 ± 1.2	17.4 ± 1.6	23.8 ± 5.0	4.333†	2		0.142		6

*F value, one-way repeated-measures ANOVA, Holm-Sidak post hoc; †χ^2 value (H), Friedman repeated-measures ANOVA on ranks, Tukey post hoc. Bold font indicates significant P values. Pre, prior to peptide application; Post, after peptide application. Note: no post hoc test was performed when $P > 0.05$.

10^{-6} M: $n = 13/16$) (Fig. 6). Concentrations below 10^{-6} M did not usually elicit a gastric mill rhythm (10^{-7}-10^{-9} M: $n = 2/31$). The Gly^1-SIFamide-elicited gastric mill rhythm included regular alternating bursting between the protractor neurons LG and IC and the retractor phase neuron VD, and presumably Int1. We did not record from Int1 but expect that it was coactive with VD due to its electrical coupling to this neuron, its synaptic inhibition from LG, and the fact that it is spontaneously active except when being inhibited (Fig. 1*B*) (Bartos et al. 1999; Nusbaum et al. 2017; White and Nusbaum 2011). The cycle period of this Gly^1-SIFamide elicited gastric mill rhythm was equivalent during 10^{-6} M and 5×10^{-6} M applications (10^{-6} M: 16.0 ± 2.15 s, $n = 6$; 5×10^{-6} M: 18.8 ± 3.38 s, $n = 12$, Mann-Whitney rank sum test: U-statistic, 26.000, $P = 0.374$). This cycle period was similar to gastric mill rhythms driven by other pathways (Blitz et al. 2004; Christie et al. 2004; White and Nusbaum 2011).

There were some aspects of the Gly^1-SIFamide-elicited gastric mill motor pattern in the isolated STG that were distinct from previously characterized versions of this rhythm. For example, during most previously studied gastric mill rhythms, the protraction phase includes GM neuron activity as well as that of LG and IC, while the retraction phase includes DG neuron activity as well as that of Int1 and VD (Beenhakker and Nusbaum 2004; Blitz et al. 2004, 2008; Christie et al. 2004). However, during gastric mill rhythms elicited by Gly^1-SIFamide (10^{-6} to 5×10^{-6} M), rhythmic bursting of the medial tooth retractor DG was common ($n = 14/19$), but it rarely alternated on a cycle-by-cycle basis with that of the protractor neurons ($n = 2/19$) (Fig. 6, *A* and *B*). During the three other applications, the DG activity was tonic instead of rhythmic (Fig. 6*C*). At the lower concentrations, in which Gly^1-SIFamide did not elicit a gastric mill rhythm, it still often activated

rhythmic bursting in the DG neuron, which remained unrelated to that in any other STG neuron (10^{-7} M, $n = 9/12$; 10^{-8} M, $n = 6/8$; 10^{-9} M, $n = 0/4$). Lastly, the medial tooth protractor GM neurons were rarely activated during these Gly^1-SIFamide-elicited gastric mill rhythms, and, when activated, their activity was weak and not sustained (5×10^{-6} M: $n = 2/8$).

Also distinct from most previous gastric mill rhythms was the presence of unusually long IC neuron bursts, which often spanned multiple pyloric cycles, during the Gly^1-SIFamide-elicited gastric mill rhythm (duration range: 0–3 s; spikes/burst range: 0–52; mean: 11.1 ± 1.7 spikes/burst, $n = 1658$ cycles, 12 preparations) (Figs. 6 and 7). As in other gastric mill rhythms, during Gly^1-SIFamide (5×10^{-6} M)-elicited gastric mill rhythms, the IC neuron was primarily active during the protraction phase, despite the continued presence of the pyloric rhythm during protraction and retraction [% pyloric cycles with IC active: protraction, $96.1 \pm 1.9\%$ (786 cycles); retraction, $46.1 \pm 7.3\%$ (846 cycles), $n = 12$]. Not all of these IC bursts were prolonged. Even within individual protraction phases, the IC bursts ranged considerably in both duration and number of spikes/burst (Fig. 6). In contrast, the IC neuron exhibited consistently modest pyloric-timed activity during saline superfusion (1.56 ± 0.5 spikes/burst, $n = 12$) (Fig. 6).

The prolonged IC bursts correlated with a slowing of the pyloric rhythm (Figs. 6–8). Specifically, in 11/12 preparations, there was a positive correlation between pyloric cycle period and IC burst duration during Gly^1-SIFamide (5×10^{-6} M) application (Pearson correlation, $r = 0.61$–0.96, $P < 0.001$). In one preparation in which the IC burst duration did not extend beyond 0.4 s during the Gly^1-SIFamide application, there was a negative correlation ($r = -0.28$, $P < 0.001$). In plots of the normalized pyloric cycle period as a function of IC burst duration, a positive correlation is more evident beginning

Table 2. *Concentration-dependent modulation of LP neuron activity by Gly[1]-SIFamide*

LP Parameter	Mean ± SE			F/H	df	P			N
	Pre	Peptide	Post			Pre vs. Peptide	Post vs. Peptide	Pre vs. Post	
Burst duration, s									
5×10^{-6}	0.35 ± 0.03	0.37 ± 0.03	0.37 ± 0.03	0.163*	10,2		0.850		11
10^{-6}	0.36 ± 0.04	0.36 ± 0.03	0.39 ± 0.03	0.866*	10,2		0.436		11
10^{-7}	0.37 ± 0.03	0.39 ± 0.03	0.36 ± 0.04	0.492*	11,2		0.618		12
10^{-8}	0.37 ± 0.03	0.34 ± 0.03	0.37 ± 0.04	0.803*	10,2		0.462		11
10^{-9}	0.32 ± 0.04	0.34 ± 0.04	0.36 ± 0.04	0.403*	5,2		0.679		6
Spike number, spikes/burst									
5×10^{-6}	5.5 ± 0.7	8.2 ± 0.7	5.8 ± 0.7	12.507*	11,2	**<0.001**	**<0.001**	0.652	12
10^{-6}	6.2 ± 0.7	8.0 ± 0.6	6.9 ± 0.6	8.399*	10,2	**0.002**	**0.046**	0.123	11
10^{-7}	6.1 ± 0.7	7.8 ± 0.7	6.9 ± 0.8	5.097*	11,2	**0.013**	0.180	0.164	12
10^{-8}	5.8 ± 0.6	5.9 ± 0.5	5.8 ± 0.6	0.019*	10,2		0.981		11
10^{-9}	5.0 ± 0.6	5.4 ± 0.8	5.3 ± 0.7	0.423*	5,2		0.666		6
Spike frequency, Hz									
5×10^{-6}	13.9 ± 1.5	20.6 ± 1.3	13.7 ± 1.2	44.778*	11,2	**<0.001**	**<0.001**	0.625	12
10^{-6}	13.9 ± 1.1	19.7 ± 1.3	14.9 ± 1.1	18.727†	2	**<0.001**	**0.015**	0.295	11
10^{-7}	13.6 ± 1.2	17.5 ± 1.3	13.5 ± 1.4	11.61*	11,2	**<0.001**	**0.001**	0.938	12
10^{-8}	13.3 ± 1.1	14.9 ± 1.0	13.4 ± 1.2	5.203*	10,2	**0.026**	**0.03**	0.325	11
10^{-9}	12.8 ± 1.7	12.8 ± 1.5	12.3 ± 1.4	0.656*	5,2		0.540		6
Phase on, % of pyloric cycle									
5×10^{-6}	37.4 ± 1.7	42.7 ± 1.2	38.4 ± 1.9	6.541*	9,2	**0.009**	**0.027**	0.511	10
10^{-6}	37.2 ± 1.8	42.0 ± 1.2	37.2 ± 1.9	7.718*	10,2	**0.006**	**0.008**	0.988	11
10^{-7}	38.1 ± 1.3	41.0 ± 1.2	38.2 ± 1.3	7.006*	11,2	**0.010**	**0.009**	0.908	12
10^{-8}	38.0 ± 1.5	41.1 ± 1.2	39.7 ± 1.3	5.768*	10,2	**0.009**	0.138	0.153	11
10^{-9}	40.4 ± 2.2	39.8 ± 3.1	93.3 ± 2.2	0.488*	5,2		0.628		6
Phase off, % of pyloric cycle									
5×10^{-6}	56.2 ± 3.3	73.2 ± 1.1	58.2 ± 2.7	30.533*	9,2	**<0.001**	**<0.001**		
10^{-6}	56.4 ± 3.0	71.6 ± 1.5	58.2 ± 3.4	13.818†	2	**0.002**	**0.008**	0.905	11
10^{-7}	57.4 ± 1.8	68.9 ± 1.7	56.7 ± 2.3	26.939*	11,2	**<0.001**	**<0.001**	0.729	12
10^{-8}	59.4 ± 3.4	64.9 ± 10.6	60.8 ± 8.0	3.655*	10,2	**0.050**	0.129	0.512	11
10^{-9}	60.2 ± 4.1	61.0 ± 5.9	59.3 ± 5.0	0.342*	5,2		0.718		6
Duty cycle, % of pyloric cycle									
5×10^{-6}	18.9 ± 2.2	30.4 ± 1.7	19.7 ± 1.9	31.245*	9,2	**<0.001**	**<0.001**	0.655	10
10^{-6}	19.3 ± 2.1	29.3 ± 2.1	21.2 ± 1.9	11.398*	10,2	**<0.001**	**0.003**	0.388	11
10^{-7}	19.3 ± 1.6	27.9 ± 2.2	18.5 ± 2.2	21.179*	11,2	**<0.001**	**<0.001**	0.641	12
10^{-8}	21.5 ± 2.3	24.0 ± 2.3	21.1 ± 1.6	1.652*	10,2		0.217		11
10^{-9}	19.8 ± 2.4	21.1 ± 3.7	47.3 ± 10.1	1.333†	2		0.570		6

*F value, one-way repeated-measures ANOVA, Holm-Sidak post hoc; †χ^2 value (H), Friedman repeated-measures ANOVA on ranks, Tukey post hoc. Bold font indicates significant P values. Pre, prior to peptide application; Post, after peptide application. Note: no post hoc test was performed when $P > 0.05$.

at IC burst durations of ~0.5 s (Fig. 7A). Highlighting this point, in 6/12 preparations there was an inflection point in the data distribution, which indicated the onset of the positive correlation between IC burst duration and pyloric cycle period (e.g., Fig. 7B) (range of IC burst duration at the inflection point: 0.46–1.15 s). Specifically, in these experiments the data points deviated from a horizontal line at IC burst durations longer than the inflection point (piecewise linear model: each of 6 preparations, $P < 0.001$) (Fig. 7). On average, this inflection point occurred when the IC burst duration was 0.70 ± 0.11 s ($n = 6$). In the other 5/12 experiments in which there was a positive correlation, there was no inflection point in the data (piecewise linear model: each of 5 preparations, $P > 0.05$) and the data were fit by a straight line (e.g., Fig. 7C).

The correlation between long IC bursts and prolonged pyloric cycle periods was primarily a feature of the protraction phase of Gly[1]-SIFamide gastric mill rhythms. In preparations with inflection points, there were few IC bursts during retraction that had durations longer than that at the inflection point ($4.1 \pm 1.9\%$ of 446 pyloric cycles, $n = 6$). In contrast, during protraction, most IC bursts were longer than the duration of bursts at the inflection point ($60.2 \pm 8.8\%$ of 395 pyloric cycles, $n = 6$).

Another relatively unique Gly[1]-SIFamide action was the prolongation of most pyloric rhythm-timed LPG neuron bursts beyond the end of the associated PD neuron burst (Fig. 8A). In *C. borealis*, the LPG neuron is electrically coupled to the pyloric pacemaker neurons AB and PD. Qualitatively, under most previously studied conditions, the rhythmic LPG bursting activity is tightly time-locked to that of these pacemaker neurons, even when the gastric mill rhythm is concurrently active (Bartos and Nusbaum 1997; Marder et al. 2017). Consistent with these previous studies, bursts in the LPG neuron primarily overlapped with coincident PD bursts when recorded during saline superfusion (e.g., Fig. 8A). Specifically, during saline superfusion before and after a Gly[1]-SIFamide application, LPG bursts extended past the coincident PD burst during only ~15% of analyzed cycles (saline: $14.8 \pm 9.5\%$; 133/805 cycles; wash: $15.7 \pm 5.1\%$; 141/841 cycles; $n = 9$). In contrast, during Gly[1]-SIFamide (5×10^{-6} M) applications, cycles in which the LPG burst extended past the PD burst increased to 90% of analyzed cycles across both protraction and retraction ($90.9 \pm 2.8\%$; 1132/1250 cycles; $n = 9$; Freidman RM-ANOVA on ranks, Tukey, $P < 0.001$ saline vs. Gly[1]-SIFamide; $P = 0.018$ Gly[1]-SIFamide vs. wash; $P = 0.613$ saline vs. wash). Moreover, when the LPG burst extended beyond the

Table 3.   *Concentration-dependent modulation of PY neuron activity by Gly[1]-SIFamide*

| PY | Mean ± SE | | | | | P | | | |
Parameter	Pre	Peptide	Post	F/H	df	Pre vs. Peptide	Post vs. Peptide	Pre vs. Post	N
Burst Duration, s									
5×10^{-6}	0.92 ± 0.17	0.32 ± 0.03	0.79 ± 0.12	14.138*	8,2	**<0.001**	**0.002**	0.288	9
10^{-6}	0.78 ± 0.12	0.31 ± 0.02	0.78 ± 0.15	15.200†	2	**0.005**	**0.001**	0.896	10
10^{-7}	0.78 ± 0.08	0.45 ± 0.05	0.81 ± 0.11	15.526*	10,2	**<0.001**	**<0.001**	0.701	11
10^{-8}	0.73 ± 0.13	0.49 ± 0.07	0.67 ± 0.09	10.364†	2	**0.004**	0.407	0.133	11
10^{-9}	0.63 ± 0.14	0.82 ± 0.36	0.85 ± 0.32	2.333†	2		0.43		6
Phase on, % of pyloric cycle									
5×10^{-6}	55.6 ± 3.5	71.2 ± 1.2	57.9 ± 2.9	14.889†	2	**<0.001**	**0.026**	0.466	9
10^{-6}	56.9 ± 2.8	70.6 ± 1.0	58.5 ± 2.9	15.200†	2	**0.001**	**0.005**	0.896	10
10^{-7}	56.7 ± 1.9	65.1 ± 1.4	57.1 ± 1.9	18.910*	10,2	**<0.001**	**<0.001**	0.816	11
10^{-8}	57.9 ± 2.9	63.0 ± 2.5	59.1 ± 2.4	3.748*	10,2	**0.0500**	0.109	0.567	11
10^{-9}	59.1 ± 4.4	58.9 ± 4.8	58.0 ± 4.3	0.306*	5,2		0.743		6
Phase off, % of pyloric cycle									
5×10^{-6}	95.9 ± 0.4	95.2 ± 0.5	95.7 ± 0.4	0.438*	8,2		0.65		9
10^{-6}	95.4 ± 0.4	95.4 ± 0.5	96.1 ± 0.2	1.151*	9,2		0.339		10
10^{-7}	95.7 ± 0.3	95.9 ± 0.2	95.9 ± 0.3	0.132*	10,2		0.877		11
10^{-8}	95.3 ± 0.3	95.8 ± 0.3	95.5 ± 0.3	1.166*	10,2		0.332		11
10^{-9}	95.2 ± 0.4	95.2 ± 0.6	94.7 ± 0.6	0.841*	5,2		0.46		6
Duty cycle, % of pyloric cycle									
5×10^{-6}	40.5 ± 3.6	25.5 ± 1.4	38.0 ± 2.9	22.658*	8,2	**<0.001**	**<0.001**	0.314	9
10^{-6}	38.5 ± 2.8	24.6 ± 1.1	37.6 ± 2.9	15†	2	**0.002**	**0.002**	1	10
10^{-7}	39.2 ± 2.1	30.8 ± 1.4	38.9 ± 2.1	16.102*	10,2	**<0.001**	**<0.001**	0.818	11
10^{-8}	37.4 ± 3.0	33.0 ± 2.6	36.5 ± 2.4	2.567*	10,2		0.102		11
10^{-9}	36.0 ± 4.2	36.5 ± 5.6	47.3 ± 10.1	0.333†	2		0.956		6

*F value, one-way repeated-measures ANOVA, Holm-Sidak post hoc; †χ^2 value (H), Friedman repeated-measures ANOVA on ranks, Tukey post hoc. Bold font indicates significant P values. Pre, prior to peptide application; Post, after peptide application. Note: no post hoc test was performed when $P > 0.05$. PY, pyloric.

coincident PD burst, the number of LPG spikes in this extended period was greater in Gly[1]-SIFamide compared with controls (saline: 0.17 ± 0.11 spikes/burst, range: 0–2 spikes; Gly[1]-SIFamide: 2.57 ± 0.3 spikes/burst, range: 0–8 spikes; wash: 0.18 ± 0.05 spikes/burst, range: 0–2 spikes; RM-ANOVA, Holm-Sidak, $P < 0.001$ saline vs. Gly[1]-SIFamide; $P < 0.001$ Gly[1]-SIFamide vs. wash; $P = 0.94$ saline vs. wash). These prolonged, pyloric-timed LPG bursts tended to be patterned by the gastric mill rhythm such that the most prolonged LPG bursts tended to alternate with the largest IC bursts ($n = 7/9$) (Fig. 8, B and C).

Thus, the gastric mill motor pattern elicited by Gly[1]-SIFamide application to the isolated STG included coactive bursting of LG and IC, which alternated with Int1 and VD neuron bursts. Additionally, LPG exhibited gastric mill rhythm-timed bouts of prolonged activity, which were consistently abbreviated during the largest IC bursts (Fig. 8). During these rhythms, the rhythmic bursting in the DG neuron was often not tightly coordinated with the gastric mill rhythm, while the GM neurons were silent.

In a few of these Gly[1]-SIFamide applications to the isolated STG, the projection neuron MCN1 was also activated, as was evident in *ion* recordings on the side of the nerve still connected to the STG (5×10^{-6} M: 3/14; 10^{-6} M: 2/8; 10^{-7} M: 0/6; 10^{-8} M: 0/7; 10^{-9} M: 0/5). This occurred despite the fact that the MCN1 soma and local branching structure in the commissural ganglion was separated from the STG. This Gly[1]-SIFamide activation of MCN1 therefore occurred either at the MCN1 axon terminals in the STG or on its axon upstream of the STG. We did not directly identify the Gly[1]-SIFamide responsive site on MCN1, but the MCN1 activity pattern provided an indicator

of the MCN1 spike initiation site. Specifically, when MCN1 activity initiates within the STG and its spiking is monitored via an *ion* recording, the MCN1 activity is eliminated during each LG burst, due to LG inhibition of MCN1$_{STG}$ (Coleman and Nusbaum 1994). In contrast, when MCN1 activity initiates upstream from the STG, its *ion*-recorded activity persists during each LG burst. In our experiments, the Gly[1]-SIFamide activated MCN1 spiking always persisted during rhythmic LG bursting ($n = 5/5$). This result suggests that either the MCN1 axon has receptors for Gly[1]-SIFamide, or it has a branching structure containing Gly[1]-SIFamide receptors within the neuropil at the anterior end of the *stn,* near the junction with the *son*s (Fig. 2) (Goaillard et al. 2004). Axons in the STNS and other systems have receptors for biogenic amines and neuropeptides through which modulators can activate alternative spike initiation zones (Bucher et al. 2003; Bucher and Goaillard 2011; Goaillard et al. 2004; Meyrand et al. 1992; Städele and Stein 2016).

MCN5 Stimulation Includes Gly[1]-SIFamide-like Actions on the Gastric Mill Circuit

Insofar as MCN5 contains Gly[1]-SIFamide (Fig. 4), and applying this peptide to the STG excited the pyloric rhythm and elicited a gastric mill rhythm (Figs. 5 and 6), we assessed the ability of MCN5 stimulation to mimic these Gly[1]-SIFamide actions. In a previous study, relatively brief (5–10 s) MCN5 stimulation influenced the pyloric rhythm but did not activate a gastric mill rhythm (Norris et al. 1996). The dominant effect of these brief MCN5 stimulations was excitation of the pyloric pacemaker neurons and ionotropic inhibition of the nonpacemaker neurons. Some metabotropic actions were suggested by the prolonging of the LPG neuron burst beyond that of the
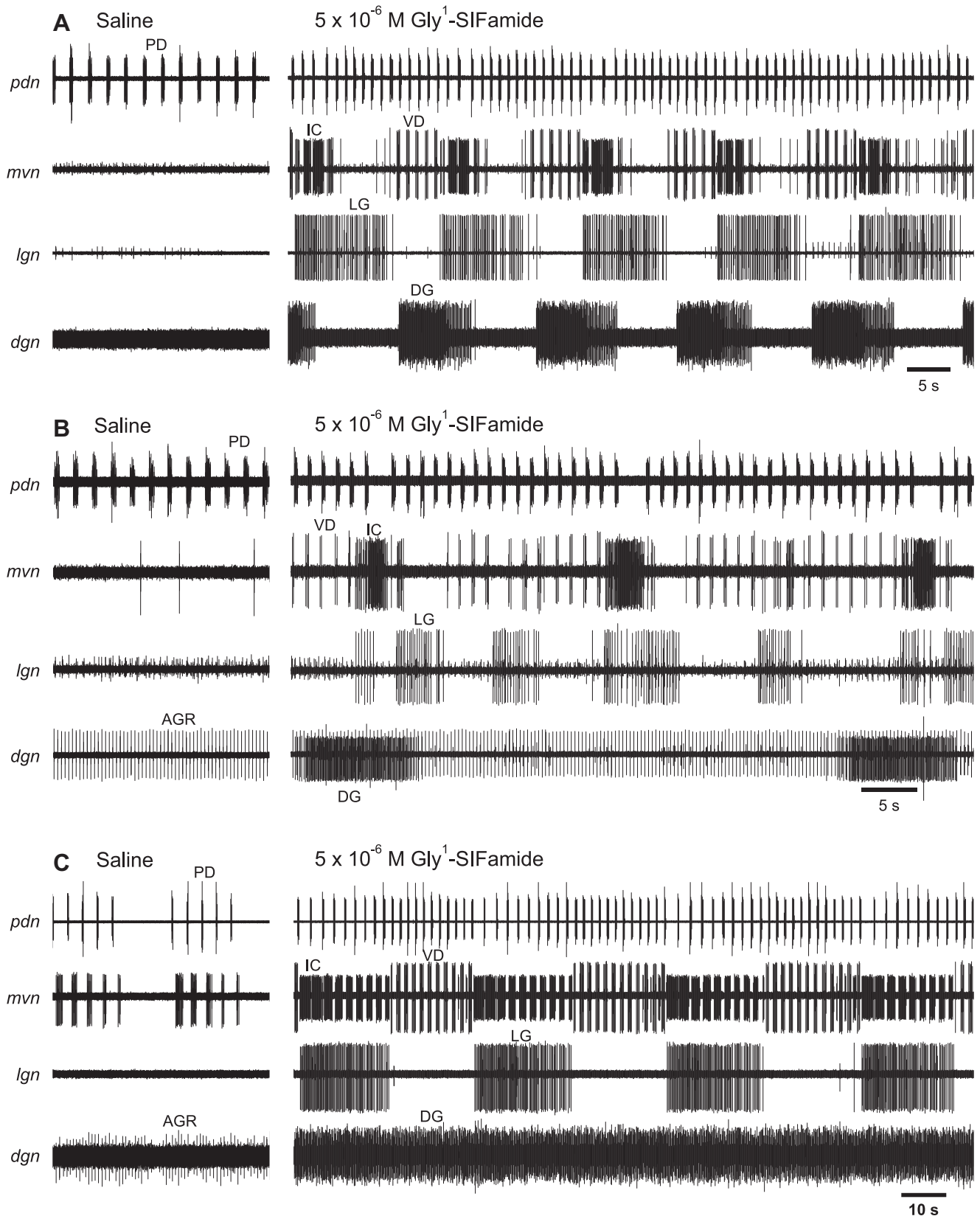
Fig. 6. Gly[1]-SIFamide elicits a novel gastric mill rhythm in the isolated *C. borealis* STG. In saline, there was commonly an ongoing pyloric rhythm, evident from the PD bursting (*pdn*), little to no activity in IC (*mvn*), and no VD (*mvn*), LG (*lgn*), or DG activity (*dgn*). Gly[1]-SIFamide (5×10^{-6} M) elicited a gastric mill rhythm that included activation of VD, LG, and DG as well as prolonged IC bursts. However, there was variability in the pattern between preparations. The variable patterns included regular rhythmic alternating bursting between LG and DG (*A*), irregular LG and DG bursting (*B*), and regular LG bursting with tonic DG activity (*C*). Note that, in all three sets of recordings, the pyloric rhythm slowed during each prolonged IC burst. *A–C* were recorded in different preparations.
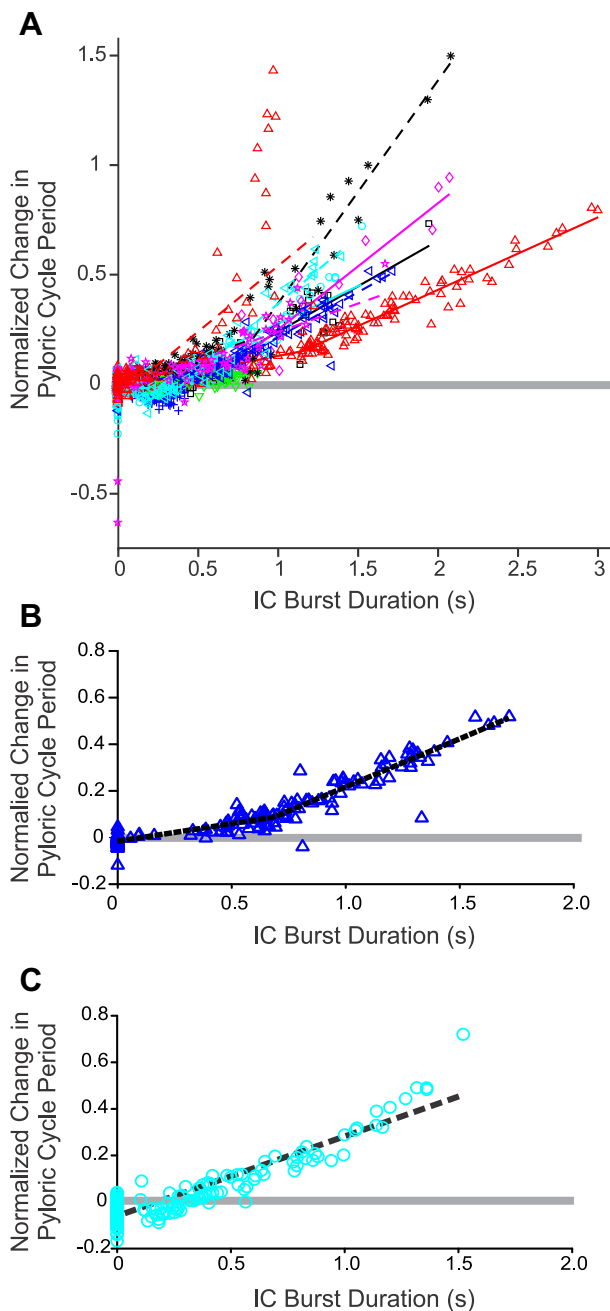
Fig. 7. Prolonged IC neuron bursts correlate with increased pyloric cycle period during the Gly^1-SIFamide-elicited gastric mill rhythm. *A*: the change in pyloric rhythm cycle period during the protraction phase of the gastric mill rhythm, normalized to that occurring during the retraction phase when the IC neuron is not active, is plotted as a function of IC neuron burst duration ($n = 1,658$ cycles, 12 preparations). During Gly^1-SIFamide (5×10^{-6} M) the pyloric rhythm slowed (cycle period increased) when the IC neuron burst duration exceeded ~0.5 s, beyond which longer IC bursts correlate with slower pyloric rhythms. Each symbol/color combination represents cycles from a single preparation. Solid and dashed lines in corresponding colors are the fits to the data for each experiment. In some experiments the data deviated from a horizontal line at IC burst durations longer than an inflection point (piecewise linear model: $P < 0.001$, $n = 6/12$). In the other 6/12 experiments, there was no inflection point in the data (piecewise linear model: $P > 0.05$) and the data were fit by a straight line. For clarity, data and the corresponding fit line from one example experiment with a significant inflection point (*B*) and one without a significant inflection point (*C*) are plotted. Black dotted lines in *B* and *C* are the fits to the data. Gray solid lines in all graphs lines indicate no change in cycle period relative to the average cycle period during retraction cycles when IC was silent.

coactive PD neurons, as we reported above for Gly^1-SIFamide applications, and poststimulation rebound bursts in the IC and VD neurons (Norris et al. 1996). Here, we used longer-lasting MCN5 stimulation (~60–300 s, 25–35 Hz) and found that it also elicited a gastric mill rhythm.

The MCN5-elicited gastric mill rhythm exhibited some canonical features of this motor pattern as well as sharing several relatively unique features with the rhythm elicited by Gly^1-SIFamide (5×10^{-6} M) application. Among the canonical features were the rhythmic alternating bursting of protraction phase (LG, IC) and retraction phase neurons (DG,VD, and presumably Int1) (Fig. 9). These rhythms displayed a cycle period of 14.4 ± 2.3 s ($n = 4$), which was similar to that of other gastric mill rhythms (Blitz et al. 2004; Christie et al. 2004; White and Nusbaum 2011) and was comparable to the above-reported value for the Gly^1-SIFamide-elicited gastric mill rhythm (Mann-Whitney rank sum test: $P = 0.2$, Gly^1-SIFamide, $n = 12$; MCN5, $n = 4$). However, unlike the Gly^1-SIFamide-elicited gastric mill rhythms, DG activity was more consistently coordinated with the MCN5-driven gastric mill rhythm ($n = 5/7$). Also similar to the Gly^1-SIFamide gastric mill rhythm (Figs. 6 and 8), the IC neuron bursting was periodically prolonged during MCN5 stimulation (Fig. 9) well beyond what occurred for most previously characterized gastric mill rhythms in *C. borealis* (Beenhakker et al. 2004; Blitz et al. 2004, 2008; Christie et al. 2004; Coleman and Nusbaum 1994). Another distinct feature of these MCN5-driven rhythms was the presence of a third active phase, in which the LPG neurons periodically escaped from the pyloric rhythm and fired a prolonged burst that spanned several pyloric cycles following each DG neuron burst ($n = 6$) (Fig. 9). This extension of LPG activity beyond PD bursts was similar to Gly^1-SIFamide actions on LPG although, as indicated above for the DG neuron, the patterning of this LPG activity was distinct between the Gly^1-SIFamide- and MCN5-elicited rhythms (Figs. 8 and 9). The resulting MCN5-elicited gastric mill motor pattern thus tended to include sequential bursting of LG/IC, followed by DG/VD/Int1, and then the LPG burst, after which the VD and LPG neurons displayed pyloric rhythm-timed activity until the next LG/IC burst (Fig. 9).

Also similar to the Gly^1-SIFamide-elicited gastric mill rhythm was that the prolonged IC neuron bursts during the MCN5-elicited gastric mill rhythm influenced the pyloric rhythm (Fig. 9). Specifically, there was a positive correlation between pyloric cycle period and IC burst duration (Pearson correlation, $r = 0.42$–0.87, $P < 0.001$, $n = 4/4$).

MCN5 Activity Pattern Is Regulated by STG Circuit Feedback

Bath-applied modulator does not always mimic the actions of neuronally released modulator (Marder 2012; Nusbaum et al. 2017). Insofar as this was also the case for the actions of Gly^1-SIFamide application and MCN5 stimulation on the STG microcircuits, we sought to identify potential sources for their differences. One factor that can contribute to these differences is that long-distance and local feedback can shape the temporal structure of the neuronal release of a modulator (Bartos et al. 1999; Blitz and Nusbaum 2008; Coleman et al. 1995; Nusbaum et al. 2017). Previous studies (Blitz and Nusbaum 2012; Norris

Fig. 8. The Gly[1]-SIFamide-elicited gastric mill rhythm includes alternating, prolonged bursting in the IC and LPG neurons. *A, left*: In saline, PD and LPG bursts had a similar duration (*pdn, lpgn*; unfilled arrows, red boxes) during a pyloric rhythm. (*A, right*) Gly[1]-SIFamide (5×10^{-6} M) application activated a gastric mill rhythm that included alternating bursting in LG (*lgn*) and DG (*dgn*). Additionally, after each set of prolonged IC bursts, several successive LPG bursts extended beyond the coincident PD burst (filled arrows, red boxes), followed by shorter LPG bursts that were similar in duration to the coincident PD bursts (unfilled arrows, red boxes). *B*: the number of LPG spikes/burst extending beyond each coincident PD burst (gray histogram) and the number of IC spikes/burst (black-outlined histogram) are plotted against pyloric cycle number during Gly[1]-SIFamide (5×10^{-6} M) application from the experiment in *A*. Note that the greatest number of LPG spikes extending beyond PD alternated with the greatest number of IC spikes/burst. *C*: the average percent of cycles with LPG spikes extending beyond PD are plotted for cycles in which the number of IC spikes/burst was 0–5, 6–25, and >25. During the shortest IC bursts (0–5 spikes per burst), LPG fired 2–8 spikes (black bar) beyond the coincident PD burst in most pyloric cycles. In contrast, during the longest IC bursts (>25 spikes), LPG fired 0–1 spikes (white bar) beyond each coincident PD burst in most pyloric cycles. Matching letters above the bars indicate significant differences between groups (one-way RM-ANOVA, Holm-Sidak post hoc; $P < 0.05$). Spks, spikes.
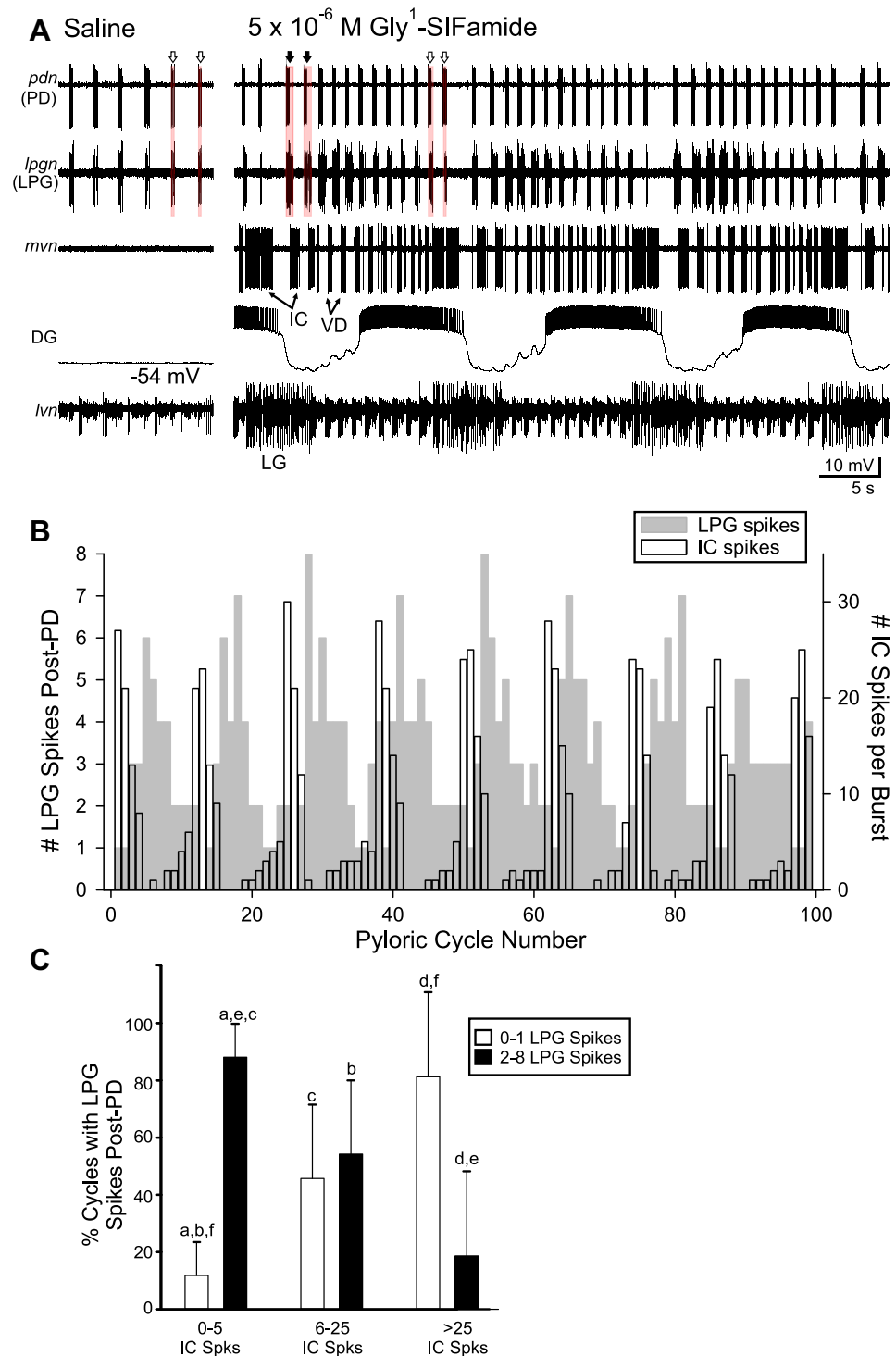
et al. 1996) established that the MCN5 activity pattern is regulated by long distance feedback inhibition from the pyloric pacemaker neuron AB onto MCN5 in the CoG, resulting in MCN5 commonly exhibiting a pyloric rhythm-timed activity pattern. This pyloric-timed pattern is further modified in the CoG during some gastric mill rhythms (Beenhakker and Nusbaum 2004; Blitz and Nusbaum 2008; Norris et al. 1996). In this study, however, we used tonic stimulation of MCN5 and thereby bypassed the ability of long-distance feedback to regulate the MCN5 activity pattern. Here, we examined

whether there was local synaptic feedback onto the MCN5 axon terminals in the STG, which might also regulate MCN5 (co)transmitter release. This possibility was examined using intra-axonal MCN5 recordings within ~50 μm of the STG neuropil (designated as MCN5$_{STG}$), as done previously for the comparable MCN1$_{STG}$ recordings (Coleman and Nusbaum 1994; Nusbaum et al. 1992) (see MATERIALS AND METHODS). These intra-axonal recordings were sufficiently close, electrotonically, to the STG neuropil to enable the recording of unitary postsynaptic potentials (PSPs; Fig. 10).
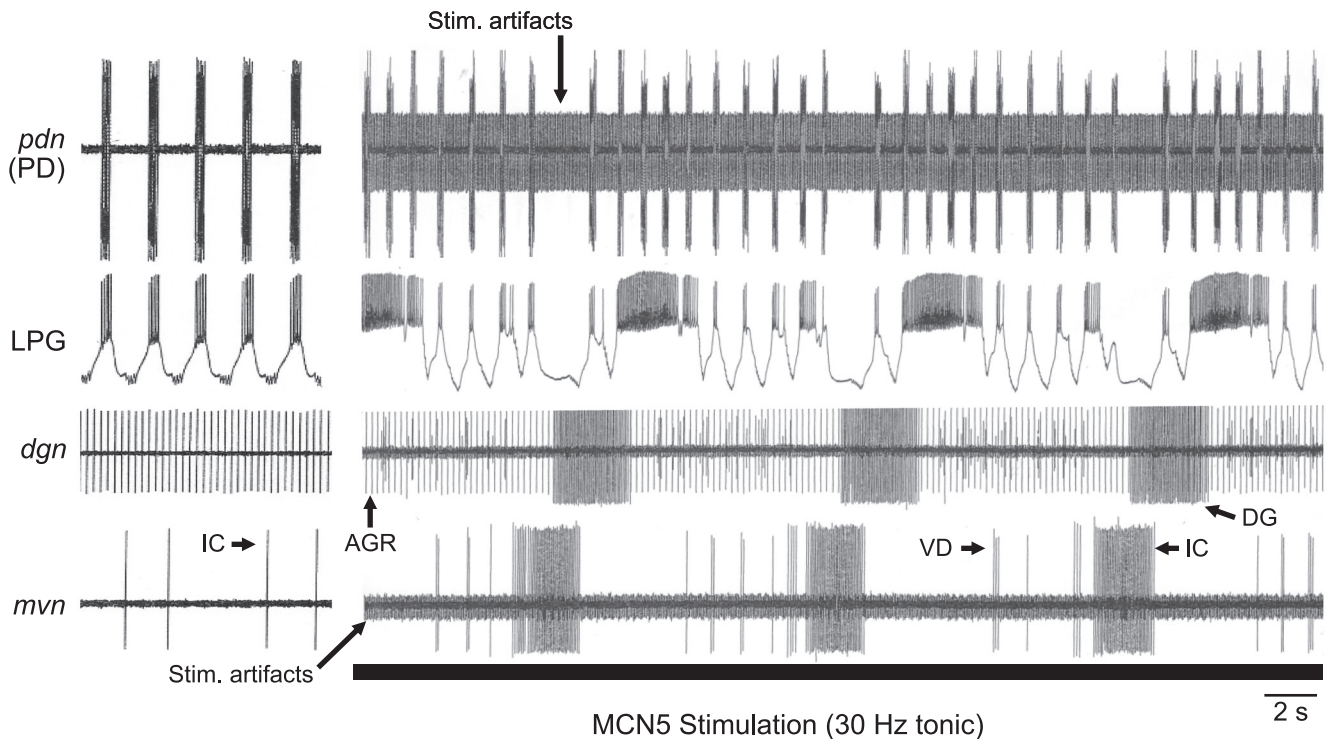
Fig. 9. MCN5 stimulation elicits a Gly[1]-SIFamide-like gastric mill rhythm. *Left*: in control, PD and LPG bursts had similar burst durations. DG was silent and IC was only weakly active. *Right*: tonic MCN5 stimulation (30 Hz) elicited a gastric mill rhythm with three distinct phases. Prolonged IC bursts were followed by DG bursts and then prolonged LPG bursts. Between the prolonged LPG bursts, LPG burst durations were more similar to the coincident PD burst durations (*pdn*). Similar to the Gly[1]-SIFamide rhythm, during the MCN5-driven gastric mill rhythm the pyloric cycle period (PD onset to PD onset) was increased in each cycle with a prolonged IC burst. AGR is a sensory neuron that is often spontaneously active in vitro (Städele and Stein 2016). Stim., stimulation.

Recordings from $MCN5_{STG}$ revealed that, in the absence of any experimental manipulations, its local membrane potential underwent pyloric rhythm-timed, subthreshold slow wave oscillations. Each of these pyloric-timed events included a barrage of inhibitory postsynaptic potentials (IPSPs) that were time-locked to action potentials in a PY neuron ($n = 5$) (Fig. 10A). This synaptic action was most readily evident when it was not overlaid on the MCN5 activity pattern generated in the CoG. Therefore, we performed these experiments during times when $MCN5_{CoG}$ was not initiating action potentials. Across multiple PY neuron-spike triggered sweeps, there was a consistent hyperpolarization recorded in $MCN5_{STG}$ in one such experiment. These PY-timed unitary IPSPs in $MCN5_{STG}$ had a synaptic latency of 3 ms, which is consistent with previously established direct ionotropic synaptic actions in this system (Fig. 10B) (Blitz and Nusbaum 2008; Coleman et al. 1995; Nusbaum and Marder 1989b).

We determined that the PY-timed IPSPs in $MCN5_{STG}$ were effective in regulating local MCN5 spiking. In these experiments, we injected depolarizing current into $MCN5_{STG}$ to initiate spiking in the STG, as was done previously to study local synaptic regulation of the MCN1 axon terminals (Coleman and Nusbaum 1994). Despite injecting constant amplitude depolarizing current into $MCN5_{STG}$, the MCN5 activity pattern was not tonic but instead was pyloric rhythm-timed ($n = 5/5$) (Fig. 10, C and D). This pyloric-timed $MCN5_{STG}$ pattern was characterized by a cessation of $MCN5_{STG}$ spiking during the PY neuron phase of each pyloric cycle; this contrasts with the pyloric pacemaker (AB) neuron-timed suppression of MCN5 spiking when it originates in the CoG (Blitz and Nusbaum

2012; Norris et al. 1996). Furthermore, increasing the PY neuron firing rate by intracellular current injection reduced or eliminated $MCN5_{STG}$ activity ($n = 4$), while suppressing PY neuron activity by hyperpolarizing current injection changed $MCN5_{STG}$ activity from pyloric-timed to tonic ($n = 3$) (Fig. 10, C and D). These results suggest that when MCN5 spiking originates in the CoG, its (co)transmitter release in the STG is limited to one-third of each pyloric cycle, when LP/IC are active. This is because local inhibition of the $MCN5_{STG}$ terminals during the PY phase and long-distance feedback inhibition during the AB/PD/LPG phase can prevent and/or decrease transmitter release.

DISCUSSION

In this study we showed that Gly[1]-SIFamide has concentration-specific excitatory actions on the pyloric rhythm in the isolated *C. borealis* STG and, at relatively high concentrations, activates a novel gastric mill rhythm that includes prolonged IC and LPG neuron activity. We also established the presence of Gly[1]-SIFamide-IR throughout the STNS of *C. borealis*, including within the axon terminals of two pairs of CoG projection neurons that innervate the STG. We determined that one of these projection neurons is MCN5, which influences the pyloric rhythm by enhancing pyloric pacemaker neuron activity and providing ionotropic inhibition to the nonpacemaker neurons (Norris et al. 1996). As shown here, MCN5 also mimics at least some Gly[1]-SIFamide actions by extending the activity of the IC and LPG neurons and eliciting a novel, Gly[1]-SIFamide-like gastric mill rhythm. The prolonged LPG bursting results in its activity periodically diverging from that of the PD neurons, to
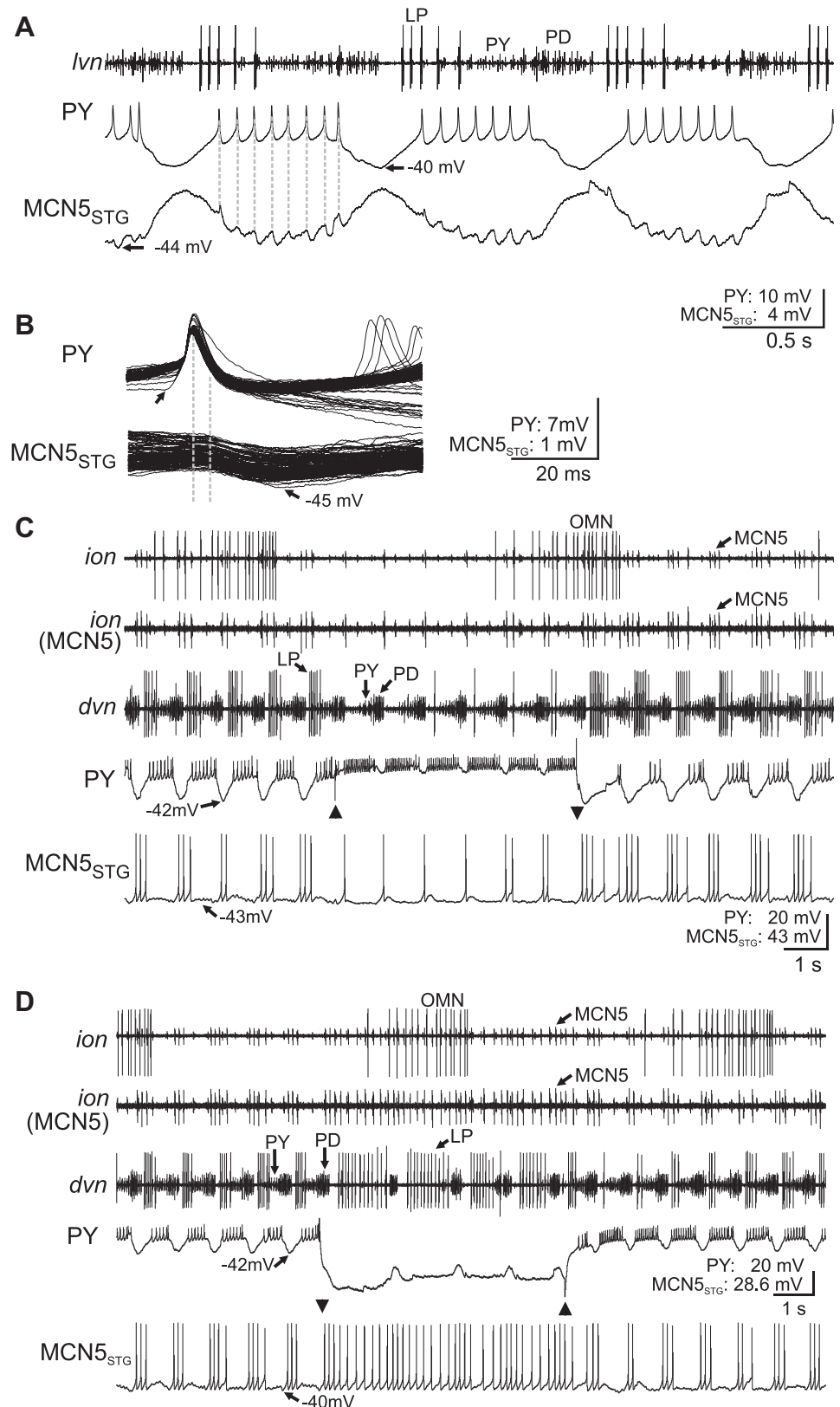
Fig. 10. The pyloric PY neuron provides presynaptic inhibition to the STG terminals of MCN5. *A*: during an ongoing pyloric rhythm, evident in the extracellular *lvn* recording, there were rhythmic oscillations in the MCN5$_{STG}$ membrane potential. During the PY phase of this rhythm, MCN5$_{STG}$ was hyperpolarized and exhibited hyperpolarizing inhibitory postsynaptic potentials (IPSPs) that appeared to coincide with PY action potentials (dashed lines). *B*: overlaid spike triggered sweeps (109 sweeps) reveal unitary IPSPs from a PY neuron to MCN5$_{STG}$. Gray dashed lines indicate the distance measured as the synaptic latency. *C*: depolarizing current injection into a PY neuron (between arrowheads) increased its firing rate and reduced MCN5$_{STG}$ activity. MCN5 activity was initiated locally through constant amplitude depolarizing current injection into MCN5$_{STG}$. The local MCN5 action potentials propagated antidromically, toward the MCN5 soma through the *ion*. *D*: hyperpolarizing current injected into one PY neuron (between arrowheads) suppressed its activity as well as that in the other, electrically coupled PYs (*dvn*) and changed the MCN5$_{STG}$ activity pattern from pyloric-timed to tonic. LP spikes per burst also decreased (*C*) and increased (*D*) due to PY depolarization and hyperpolarization, respectively. The change in LP activity was due to an established inhibitory synapse from PY to LP (Marder and Bucher 2007). In *C* and *D*, action potentials in the oesophageal motor neuron (OMN) were digitally removed in each of the lower copies of the *ion* recording to improve visibility of MCN5 action potentials. MCN5$_{STG}$, MCN5 axon near the entrance to the STG.

which it is electrically coupled. These results support the hypothesis that Gly[1]-SIFamide is a peptide transmitter used by MCN5 to modulate circuit output in the STG.

For some neuropeptides, there is variability in the family member(s) present across species (Chen et al. 2014; Christie et al. 2010; Jiang et al. 2012; Ma et al. 2009; Nässel 1999; Nässel and Wegener 2011; Ohno et al. 2017; Schlegel et al. 2016; Verleyen et al. 2009; Zatylny-Gaudin and Favrel 2014). With respect to SIFamide peptides, the same isoform is common across a number of insect species, with just a single amino acid

variation in the few other identified isoforms (Verleyen et al. 2009). Among the decapod species examined, all contain Gly[1]-SIFamide except the American and European lobsters *H. americanus* and *H. gammarus*, which instead contain Val[1]-SIFamide (Christie et al. 2006; Dickinson et al. 2008a; Stemmler et al. 2007). The general distribution of Gly[1]-SIFamide and Val[1]-SIFamide profiles in the STNS of *C. borealis* and *H. americanus* is nevertheless comparable, although different in detail (Christie et al. 2006; Dickinson et al. 2008a). For example, using the same antiserum as in the present study, Christie et al. (2006) observed a similar SIF-IR distribution in *H. americanus*, but with a larger number of labeled somata and axons and more extensive neuropilar processes.

Physiological Actions of Gly[1]-SIFamide on the STG Circuits

Different neuromodulators configure different pyloric rhythms in the isolated *C. borealis* STG (Marder 2012). Some of them, including Gly[1]-SIFamide as shown here, also elicit different pyloric rhythms when bath applied at different concentrations (Christie et al. 2006; Flamm and Harris-Warrick 1986; Saideman et al. 2006). Concentration-specific actions of exogenously applied peptide also occur in other rhythmic motor systems such as the lobster cardiac ganglion, the midshipman fish vocal circuit, and the crayfish swimmeret system (Braun and Mulloney 1993; Dickinson et al. 2015; Fort et al. 2007; Goodson and Bass 2000). Neuronally released peptides likely also have a range of effects due to peptide release varying across physiological firing rates (Nusbaum et al. 2017; Cropper et al. 2018b). Furthermore, concentration specific peptide actions, such as those of Gly[1]-SIFamide in the STG, might result in yet more variations in the circuit response when the peptide is neuronally released. Specifically, different circuit responses at any particular neuronal firing rate and pattern could occur because the resulting extracellular peptide concentration may not necessarily be the same near all receptors, due to peptide diffusion and extracellular peptidase-mediated cleavage (Cropper et al. 2018b; Nusbaum et al. 2017).

Well-defined neural circuits are also instructive for assessing the extent to which circuits and their regulation are conserved across related species. For example, the same modulator and/or modulatory neuron does not always act comparably on the gastric mill and/or pyloric rhythms in different decapod crustaceans (Dickinson et al. 2008b; Marder and Bucher 2007; Meyrand et al. 2000; Nusbaum et al. 2017). In some cases, the same modulator does not influence the same circuit across all related species, perhaps due to different behavioral requirements. For instance, serotonergic modulation of a swimming circuit occurs in multiple molluscan species that generate a particular swim version, but not in a mollusc that does not swim in that manner (Lillvis and Katz 2013). Similarly, the pyloric circuit in a kelp crab with a limited diet does not respond to a number of modulators that alter the pyloric rhythm in other species which have more varied diets (Dickinson et al. 2008b; Donahue et al. 2009; Stehlik 1993).

Here, we found distinctions in the pyloric rhythm response to Gly[1]-SIFamide application in *C. borealis* relative to Val[1]-SIFamide in *H. americanus* (Christie et al. 2006). For example, bath-applied Val[1]-SIFamide only transiently excites the lobster pyloric rhythm, while this excitation persisted for the duration

of each application in the crab. Additionally, while these peptides share concentration-specific actions on the pyloric rhythm, the Val[1]-SIFamide effects in lobster have a 10-fold higher threshold concentration and primarily affect the pyloric pacemaker neurons (Christie et al. 2006), whereas Gly[1]-SIFamide in the crab enhanced activity in the pacemaker neurons as well as the LP, IC, and PY neurons. These results reinforce the conclusions from other systems that one should extrapolate with caution both the circuit construct and the likely impact of modulator actions on circuit operation across even closely related animal groups (Gunaratne et al. 2017; Katz 2016; Sakurai and Katz 2017).

Bath Application Versus Neuronal Release

The STG microcircuits are modulated by many different locally released and circulating peptides, some of which influence the STG via both routes (Dickinson et al. 2016; Marder 2012; Marder et al. 2014; Nusbaum et al. 2017; Stein 2017). The presence of Gly[1]-SIFamide-IR in the STG terminals of two projection neurons, including MCN5, supports a locally released (co)transmitter role for Gly[1]-SIFamide. Based on this study, a likely role of Gly[1]-SIFamide as a peptide transmitter is to enable MCN5 to excite the pyloric- and gastric mill circuits. The fact that the gastric mill rhythms elicited by Gly[1]-SIFamide application and MCN5 stimulation were not identical is not surprising. This distinction is shared with most actions of the other five identified peptidergic neurons that modulate the STG circuits. Each of these neurons has at least one cotransmitter, and for only one of them (MPN, modulatory proctolin neuron) does peptide bath application mimic an STG circuit response to stimulating the related, peptidergic neuron (Blitz et al. 1999; Christie et al. 2004; DeLong et al. 2009; Nusbaum et al. 2001, 2017; Skiebe and Schneider 1994; Szabo et al. 2011). Similarly, it is likely that the ionotropic inhibitory actions of MCN5 on pyloric neurons are not mediated by Gly[1]-SIFamide, because we recorded no inhibitory actions when applying this peptide to the STG. Additionally, peptide-mediated ionotropic actions are uncommon (Nusbaum et al. 2017). This inhibition is instead likely mediated by an unidentified small molecule cotransmitter.

The mismatch between applied and neuronally released peptide can also result from their differential regulation and access to receptors. For example, in contrast to bath-applied peptide, neuronally released peptide likely has unequal access to all of its receptors and can be regulated by synaptic input, as well as commonly being coreleased with one or more cotransmitters (Granger et al. 2017; Nässel 2018; Nusbaum et al. 2017). Also, unlike the continual presence of bath-applied Gly[1]-SIFamide, the MCN5-released Gly[1]-SIFamide was not likely released in the continuous pattern suggested by our tonic MCN5 stimulation pattern, because its STG terminals received rhythmic synaptic inhibition from the pyloric PY neurons. Lastly, the effects of bath-applied Gly[1]-SIFamide are likely to reflect aspects of the actions of both MCN5 and the second, not yet identified Gly[1]-SIFamide-IR projection neuron that innervates the STG.

The Gly[1]-SIFamide- and MCN5-elicited gastric mill rhythms share several aspects that differ from most previously described gastric mill rhythms (Beenhakker and Nusbaum 2004; Blitz et al. 2004, 2008; Christie et al. 2004). These distinctions include the

unusually long IC neuron bursts and the correlated slowing of the pyloric rhythm, and the gastric mill rhythm-timed LPG neuron activity. Prolonged IC neuron bursting does also occur, and slows the pyloric rhythm, in *C. borealis* in response to stimulating the proctolinergic projection neuron MCN7 (Blitz et al. 1999). However, bath-applied proctolin in the isolated *C. borealis* STG rarely elicits either a gastric mill rhythm or such prolonged IC neuron bursting, and stimulating either of the other two proctolinergic projection neurons (MCN1, MPN) that innervate the STG does not elicit these prolonged IC neuron bursts (Blitz et al. 1999; Marder et al. 1986; Nusbaum and Marder 1989b). These results suggest the presence of an additional MCN7 cotransmitter, which could be Gly[1]-SIFamide given the similarity of their influence on the IC neuron, the presence of Gly[1]-SIFamide-IR in one *son* axon and the fact that the MCN7 axon projects through the *son* to innervate the STG (Blitz et al. 1999).

Neuronal Switching

In all previous modulation studies in *C. borealis*, the LPG neuron did not exhibit a gastric mill rhythm-timed activity pattern, despite regularly exhibiting conjoint gastric mill- and pyloric rhythm-timed patterns in the lobsters *H. americanus* and *Panulirus interruptus* (Beenhakker and Nusbaum 2004; Blitz et al. 1999; Marder and Bucher 2007; Nusbaum et al. 2017). In contrast, both Gly[1]-SIFamide application and MCN5 stimulation enabled LPG to coordinately exhibit both gastric mill- and pyloric rhythm-timed activity patterns. Several other STG microcircuit neurons in *C. borealis* also display this dual activity pattern (Weimann et al. 1991; Weimann and Marder 1994). Interestingly, a Gly[1]-SIFamide- and MCN5-like gastric mill rhythm, including the LPG burst enhancement, also resulted from stimulating an unidentified pathway in the *C. borealis* circumoesophageal connective (Weimann et al. 1991). Insofar as the axons projecting through this connective innervate the CoGs (Blitz et al. 2008; Kirby and Nusbaum 2007), this stimulated pathway may well have elicited this rhythm by activating MCN5.

The ability of neurons to switch their participation between circuits is a component of network flexibility in many rhythmic networks (Jacobs et al. 2007; Larson et al. 1994; Steriade et al. 1993; Weimann et al. 1991; Weimann and Marder 1994). In addition to MCN5/Gly[1]-SIFamide, other modulatory inputs and neuromodulators can drive switches in neuronal participation in the STNS (Blitz et al. 2008; Dickinson et al. 1990; Faumont et al. 2005; Hooper and Moulins 1989). Network level analyses suggest that modulatory inputs also regulate neuronal switching in larger scale vertebrate networks (Bouret and Sara 2005; Hermans et al. 2011). Unlike these larger systems, however, the smaller scale of invertebrate networks such as the pyloric and gastric mill networks and the smaller populations of modulatory neurons such as MCN5 enable cellular level analyses of such network reconfigurations.

In *C. borealis*, LPG is typically active with the pyloric rhythm, displaying coincident activity with its electrically coupled partners, the AB and PD neurons (Marder et al. 2017; Nusbaum et al. 2017). The periodically prolonged LPG bursting found in this study raises the possibility that MCN5 stimulation and bath-applied Gly[1]-SIFamide alter electrical coupling strength among LPG, PD, and AB. Electrical synapses are prevalent throughout microcircuits, where they can add significant complexity to circuit function, and they are often modulated (Connors and Long 2004; Marder et al. 2017; Nadim and Bucher 2014; O'Brien 2014; Pereda et al. 2013). Thus far, most examples of modulation of electrical coupling have involved the metabotropic actions of biogenic amines (e.g., serotonin and dopamine) or small molecule transmitters (e.g., glutamate) (Coulon and Landisman 2017; Johnson et al. 1993; Lane et al. 2018; O'Brien 2014; Pereda et al. 2013). Further studies would be necessary to determine how MCN5 and Gly[1]-SIFamide enable LPG to periodically separate from the fast rhythmic bursting pattern it shares with its electrically coupled partners (AB/PD neurons) and generate prolonged gastric mill-timed activity. Thus, in additional to enabling further study of the cellular mechanisms by which a modulatory neuron regulates neuronal switching, MCN5/Gly[1]-SIFamide provides an opportunity to investigate potential peptidergic modulation of electrical coupling within a functional context.

The aforementioned periodic expansion of IC neuron activity during Gly[1]-SIFamide- and MCN5-elicited gastric mill protraction is an additional example of a neuron switching its participation from pyloric-only to pyloric- and gastric mill network participation. Additionally, the slowing of the pyloric rhythm that occurs during each gastric mill-timed IC burst provides a cautionary tale regarding extrapolating phenomenological events to underlying mechanisms. Specifically, the pyloric rhythm is also slowed during protraction in gastric mill rhythms driven by the projection neuron MCN1 (Bartos and Nusbaum 1997). However, this latter rhythm does not include prolonged IC neuron bursting and the slowed pyloric rhythm results instead from the gastric mill protractor neuron LG inhibition of the MCN1 axon terminals (Bartos and Nusbaum 1997; Coleman and Nusbaum 1994). These parallel actions via distinct mechanisms suggest a need to maintain this coordination pattern under different circumstances. Behavioral coordination via intercircuit regulation occurs in many systems, such as the linkage between respiration and locomotion, and whisking and locomotion (Bartos et al. 1999; Bernasconi and Kohl 1993; Cao et al. 2012; Gravel et al. 2007; Saunders et al. 2004; Wood et al. 2004), although in most cases the underlying mechanisms remain to be determined.

Conclusions

Peptidergic neurons are pervasive across the animal kingdom, and their influence on behavior has been elucidated in many systems (Komuniecki et al. 2014; Marder 2012; Nusbaum et al. 2017; Nusbaum and Blitz 2012; Qiu et al. 2016; Taghert and Nitabach 2012; van den Pol 2012). There remain few examples, however, where elucidation of the cellular and synaptic mechanisms underlying this modulation has been achieved (Cropper et al. 2018a; Marder 2012; Nusbaum et al. 2017). In this work, we have taken advantage of the well-defined stomatogastric system to localize the dodecapeptide Gly[1]-SIFamide to the identified projection neuron MCN5, and determine its influence on the feeding-related gastric mill and pyloric circuits in the crab *C. borealis*. The fact that some of the circuit responses were similar when this peptide was applied and when MCN5 was stimulated support a neurotransmitter role for Gly[1]-SIFamide in the crab STG. Our results thus extend the literature

on the SIFamide peptide family from previous identification, distribution, and behavioral studies into the realm of its physiological actions. Future identification of the small molecule transmitter in MCN5 may enable subsequent determination of how this neuron uses its cotransmitter complement to alter STG circuit activity, a level of understanding thus far attained for only a small number of such neurons.

GLOSSARY

MCN5   modulatory commissural neuron 5

Ganglia

CoG   commissural ganglion
OG   oesophageal ganglion
STG   stomatogastric ganglion
TG   thoracic ganglion

Nerves

coc   circumoesophageal connective
dgn   dorsal gastric nerve
ion   inferior oesophageal nerve
lpgn   lateral posterior gastric nerve
lvn   lateral ventricular nerve
mgn   medial gastric nerve
mvn   medial ventricular nerve
on   oesphageal nerve
pdn   pyloric dilator nerve
stn   stomatogastric nerve
son   superior oesophageal nerve

Neurons

Pyloric

AB   anterior burster
LP   lateral pyloric
LPG   lateral posterior gastric
PD   pyloric dilator
PY   pyloric

Gastric mill

AM   anterior median
DG   dorsal gastric
GM   gastric mill
LG   lateral gastric

Gastro-pyloric

IC   inferior cardiac
Int1   interneuron 1
MG   medial gastric
VD   ventricular dilator

Sensory

AGR   anterior gastric receptor

DISCLOSURES

No conflicts of interest, financial or otherwise, are declared by the authors.

AUTHOR CONTRIBUTIONS

D.M.B., A.E.C., P.S.D., and M.P.N. conceived and designed research; D.M.B., A.E.C., A.P.C., and P.S.D. performed experiments; D.M.B., A.E.C., A.P.C., P.S.D., and M.P.N. analyzed data; D.M.B., A.E.C., A.P.C., P.S.D., and M.P.N. interpreted results of experiments; D.M.B., A.E.C., and A.P.C. prepared figures; D.M.B., A.E.C., P.S.D., and M.P.N. drafted manuscript; D.M.B., A.E.C., A.P.C., P.S.D., and M.P.N. edited and revised manuscript; D.M.B., A.E.C., A.P.C., P.S.D., and M.P.N. approved final version of manuscript.

REFERENCES

Bartos M, Manor Y, Nadim F, Marder E, Nusbaum MP. Coordination of fast and slow rhythmic neuronal circuits. *J Neurosci* 19: 6650–6660, 1999. doi:10.1523/JNEUROSCI.19-15-06650.1999.

Bartos M, Nusbaum MP. Intercircuit control of motor pattern modulation by presynaptic inhibition. *J Neurosci* 17: 2247–2256, 1997. doi:10.1523/JNEUROSCI.17-07-02247.1997.

Beenhakker MP, Blitz DM, Nusbaum MP. Long-lasting activation of rhythmic neuronal activity by a novel mechanosensory system in the crustacean stomatogastric nervous system. *J Neurophysiol* 91: 78–91, 2004. doi:10.1152/jn.00741.2003.

Beenhakker MP, Nusbaum MP. Mechanosensory activation of a motor circuit by coactivation of two projection neurons. *J Neurosci* 24: 6741–6750, 2004. doi:10.1523/JNEUROSCI.1682-04.2004.

Bernasconi P, Kohl J. Analysis of co-ordination between breathing and exercise rhythms in man. *J Physiol* 471: 693–706, 1993. doi:10.1113/jphysiol.1993.sp019923.

Blitz DM, Beenhakker MP, Nusbaum MP. Different sensory systems share projection neurons but elicit distinct motor patterns. *J Neurosci* 24: 11381–11390, 2004. doi:10.1523/JNEUROSCI.3219-04.2004.

Blitz DM, Christie AE, Coleman MJ, Norris BJ, Marder E, Nusbaum MP. Different proctolin neurons elicit distinct motor patterns from a multifunctional neuronal network. *J Neurosci* 19: 5449–5463, 1999. doi:10.1523/JNEUROSCI.19-13-05449.1999.

Blitz DM, Christie AE, Marder E, Nusbaum MP. Distribution and effects of tachykinin-like peptides in the stomatogastric nervous system of the crab, *Cancer borealis*. *J Comp Neurol* 354: 282–294, 1995. doi:10.1002/cne.903540209.

Blitz DM, Nusbaum MP. State-dependent presynaptic inhibition regulates central pattern generator feedback to descending inputs. *J Neurosci* 28: 9564–9574, 2008. doi:10.1523/JNEUROSCI.3011-08.2008.

Blitz DM, Nusbaum MP. Modulation of circuit feedback specifies motor circuit output. *J Neurosci* 32: 9182–9193, 2012. doi:10.1523/JNEUROSCI.1461-12.2012.

Blitz DM, White RS, Saideman SR, Cook A, Christie AE, Nadim F, Nusbaum MP. A newly identified extrinsic input triggers a distinct gastric mill rhythm via activation of modulatory projection neurons. *J Exp Biol* 211: 1000–1011, 2008. doi:10.1242/jeb.015222.

Bouret S, Sara SJ. Network reset: a simplified overarching theory of locus coeruleus noradrenaline function. *Trends Neurosci* 28: 574–582, 2005. doi:10.1016/j.tins.2005.09.002.

Braun G, Mulloney B. Cholinergic modulation of the swimmeret motor system in crayfish. *J Neurophysiol* 70: 2391–2398, 1993. doi:10.1152/jn.1993.70.6.2391.

Bucher D, Goaillard J-M. Beyond faithful conduction: short-term dynamics, neuromodulation, and long-term regulation of spike propagation in the axon. *Prog Neurobiol* 94: 307–346, 2011. doi:10.1016/j.pneurobio.2011.06.001.

Bucher D, Thirumalai V, Marder E. Axonal dopamine receptors activate peripheral spike initiation in a stomatogastric motor neuron. *J Neurosci* 23: 6866–6875, 2003. doi:10.1523/JNEUROSCI.23-17-06866.2003.

Cao Y, Roy S, Sachdev RNS, Heck DH. Dynamic correlation between whisking and breathing rhythms in mice. *J Neurosci* 32: 1653–1659, 2012. doi:10.1523/JNEUROSCI.4395-11.2012.

Chalasani SH, Kato S, Albrecht DR, Nakagawa T, Abbott LF, Bargmann CI. Neuropeptide feedback modifies odor-evoked dynamics in *Caenorhabditis elegans* olfactory neurons. *Nat Neurosci* 13: 615–621, 2010. doi:10.1038/nn.2526.

Chen R, Ouyang C, Xiao M, Li L. In situ identification and mapping of neuropeptides from the stomatogastric nervous system of *Cancer borealis*. *Rapid Commun Mass Spectrom* 28: 2437–2444, 2014. doi:10.1002/rcm.7037.

Christie AE, Baldwin DH, Marder E, Graubard K. Organization of the stomatogastric neuropil of the crab, *Cancer borealis*, as revealed by modulator immunocytochemistry. *Cell Tissue Res* 288: 135–148, 1997a. doi:10.1007/s004410050801.

Christie AE, Kutz-Naber KK, Stemmler EA, Klein A, Messinger DI, Goiney CC, Conterato AJ, Bruns EA, Hsu Y-WA, Li L, Dickinson PS. Midgut epithelial endocrine cells are a rich source of the neuropeptides APSGFLGMRamide (*Cancer borealis* tachykinin-related peptide Ia) and GYRKPPFNGSIFamide (Gly[1]-SIFamide) in the crabs *Cancer borealis, Cancer magister* and *Cancer productus*. *J Exp Biol* 210: 699–714, 2007. doi:10.1242/jeb.02696.

Christie AE, Lundquist CT, Nässel DR, Nusbaum MP. Two novel tachykinin-related peptides from the nervous system of the crab *Cancer borealis*. *J Exp Biol* 200: 2279–2294, 1997b.

Christie AE, Pascual MG. Peptidergic signaling in the crab *Cancer borealis*: tapping the power of transcriptomics for neuropeptidome expansion. *Gen Comp Endocrinol* 237: 53–67, 2016. doi:10.1016/j.ygcen.2016.08.002.

Christie AE, Stein W, Quinlan JE, Beenhakker MP, Marder E, Nusbaum MP. Actions of a histaminergic/peptidergic projection neuron on rhythmic motor patterns in the stomatogastric nervous system of the crab *Cancer borealis*. *J Comp Neurol* 469: 153–169, 2004. doi:10.1002/cne.11003.

Christie AE, Stemmler EA, Dickinson PS. Crustacean neuropeptides. *Cell Mol Life Sci* 67: 4135–4169, 2010. doi:10.1007/s00018-010-0482-8.

Christie AE, Stemmler EA, Peguero B, Messinger DI, Provencher HL, Scheerlinck P, Hsu YW, Guiney ME, de la Iglesia HO, Dickinson PS. Identification, physiological actions, and distribution of VYRKPPFNGSIFamide (Val[1]-SIFamide) in the stomatogastric nervous system of the American lobster *Homarus americanus*. *J Comp Neurol* 496: 406–421, 2006. doi:10.1002/cne.20932.

Clark T, Hapiak V, Oakes M, Mills H, Komuniecki R. Monoamines differentially modulate neuropeptide release from distinct sites within a single neuron pair. *PloS One* 13: e0196954, 2018. doi:10.1371/journal.pone.0196954.

Coleman MJ, Meyrand P, Nusbaum MP. A switch between two modes of synaptic transmission mediated by presynaptic inhibition. *Nature* 378: 502–505, 1995. doi:10.1038/378502a0.

Coleman MJ, Nusbaum MP. Functional consequences of compartmentalization of synaptic input. *J Neurosci* 14: 6544–6552, 1994. doi:10.1523/JNEUROSCI.14-11-06544.1994.

Coleman MJ, Nusbaum MP, Cournil I, Claiborne BJ. Distribution of modulatory inputs to the stomatogastric ganglion of the crab, *Cancer borealis*. *J Comp Neurol* 325: 581–594, 1992. doi:10.1002/cne.903250410.

Connors BW, Long MA. Electrical synapses in the mammalian brain. *Annu Rev Neurosci* 27: 393–418, 2004. doi:10.1146/annurev.neuro.26.041002.131128.

Coulon P, Landisman CE. The potential role of gap junctional plasticity in the regulation of state. *Neuron* 93: 1275–1295, 2017. doi:10.1016/j.neuron.2017.02.041.

Cropper EC, Jing J, Vilim FS, Barry MA, Weiss KR. Multifaceted expression of peptidergic modulation in the feeding system of *Aplysia*. *ACS Chem Neurosci* 9: 1917–1927, 2018a. doi:10.1021/acschemneuro.7b00447.

Cropper EC, Jing J, Vilim FS, Weiss KR. Peptide cotransmitters as dynamic, intrinsic modulators of network activity. *Front Neural Circuits* 12: 78, 2018b. doi:10.3389/fncir.2018.00078.

Cuello AC, Galfre G, Milstein C. Detection of substance P in the central nervous system by a monoclonal antibody. *Proc Natl Acad Sci USA* 76: 3532–3536, 1979. doi:10.1073/pnas.76.7.3532.

DeLong ND, Beenhakker MP, Nusbaum MP. Presynaptic inhibition selectively weakens peptidergic cotransmission in a small motor system. *J Neurophysiol* 102: 3492–3504, 2009. doi:10.1152/jn.00833.2009.

Dickinson PS, Mecsas C, Marder E. Neuropeptide fusion of two motor-pattern generator circuits. *Nature* 344: 155–158, 1990. doi:10.1038/344155a0.

Dickinson PS, Qu X, Stanhope ME. Neuropeptide modulation of pattern-generating systems in crustaceans: comparative studies and approaches. *Curr Opin Neurobiol* 41: 149–157, 2016. doi:10.1016/j.conb.2016.09.010.

Dickinson PS, Sreekrishnan A, Kwiatkowski MA, Christie AE. Distinct or shared actions of peptide family isoforms: I. Peptide-specific actions of pyrokinins in the lobster cardiac neuromuscular system. *J Exp Biol* 218: 2892–2904, 2015. doi:10.1242/jeb.124800.

Dickinson PS, Stemmler EA, Cashman CR, Brennan HR, Dennison B, Huber KE, Peguero B, Rabacal W, Goiney CC, Smith CM, Towle DW, Christie AE. SIFamide peptides in clawed lobsters and freshwater crayfish (Crustacea, Decapoda, Astacidea): a combined molecular, mass spectrometric and electrophysiological investigation. *Gen Comp Endocrinol* 156: 347–360, 2008a. doi:10.1016/j.ygcen.2008.01.011.

Dickinson PS, Stemmler EA, Christie AE. The pyloric neural circuit of the herbivorous crab *Pugettia producta* shows limited sensitivity to several neuromodulators that elicit robust effects in more opportunistically feeding decapods. *J Exp Biol* 211: 1434–1447, 2008b. doi:10.1242/jeb.016998.

Diehl F, White RS, Stein W, Nusbaum MP. Motor circuit-specific burst patterns drive different muscle and behavior patterns. *J Neurosci* 33: 12013–12029, 2013. doi:10.1523/JNEUROSCI.1060-13.2013.

Donahue MJ, Nichols A, Santamaria CA, League-Pike PE, Krediet CJ, Perez KO, Shulman MJ. Predation risk, prey abundance, and the vertical distribution of three brachyuran crabs on Gulf of Maine shores. *J Crustac Biol* 29: 523–531, 2009. doi:10.1651/08-3061.1.

Faumont S, Combes D, Meyrand P, Simmers J. Reconfiguration of multiple motor networks by short- and long-term actions of an identified modulatory neuron. *Eur J Neurosci* 22: 2489–2502, 2005. doi:10.1111/j.1460-9568.2005.04442.x.

Flamm RE, Harris-Warrick RM. Aminergic modulation in lobster stomatogastric ganglion. I. Effects on motor pattern and activity of neurons within the pyloric circuit. *J Neurophysiol* 55: 847–865, 1986. doi:10.1152/jn.1986.55.5.847.

Follmann R, Goldsmith CJ, Stein W. Spatial distribution of intermingling pools of projection neurons with distinct targets: a 3D analysis of the commissural ganglia in *Cancer borealis*. *J Comp Neurol* 525: 1827–1843, 2017. doi:10.1002/cne.24161.

Fort TJ, García-Crescioni K, Agricola H-J, Brezina V, Miller MW. Regulation of the crab heartbeat by crustacean cardioactive peptide (CCAP): central and peripheral actions. *J Neurophysiol* 97: 3407–3420, 2007. doi:10.1152/jn.00939.2006.

Goaillard JM, Schulz DJ, Kilman VL, Marder E. Octopamine modulates the axons of modulatory projection neurons. *J Neurosci* 24: 7063–7073, 2004. doi:10.1523/JNEUROSCI.2078-04.2004.

Goldberg D, Nusbaum MP, Marder E. Substance P-like immunoreactivity in the stomatogastric nervous systems of the crab *Cancer borealis* and the lobsters *Panulirus interruptus* and *Homarus americanus*. *Cell Tissue Res* 252: 515–522, 1988. doi:10.1007/BF00216638.

Goodson JL, Bass AH. Forebrain peptides modulate sexually polymorphic vocal circuitry. *Nature* 403: 769–772, 2000. doi:10.1038/35001581.

Granger AJ, Wallace ML, Sabatini BL. Multi-transmitter neurons in the mammalian central nervous system. *Curr Opin Neurobiol* 45: 85–91, 2017. doi:10.1016/j.conb.2017.04.007.

Gravel J, Brocard F, Gariépy JF, Lund JP, Dubuc R. Modulation of respiratory activity by locomotion in lampreys. *Neuroscience* 144: 1120–1132, 2007. doi:10.1016/j.neuroscience.2006.10.019.

Gunaratne CA, Sakurai A, Katz PS. Variations on a theme: species differences in synaptic connectivity do not predict central pattern generator activity. *J Neurophysiol* 118: 1123–1132, 2017. doi:10.1152/jn.00203.2017.

Gutierrez GJ, Grashow RG. *Cancer borealis* stomatogastric nervous system dissection. *J Vis Exp* 25: 1–5, 2009. doi:10.3791/1207.

Hamood AW, Haddad SA, Otopalik AG, Rosenbaum P, Marder E. Quantitative reevaluation of the effects of short- and long-term removal of descending modulatory inputs on the pyloric rhythm of the crab, *Cancer borealis*. *eNeuro* 2: 1–13, 2015. doi:10.1523/ENEURO.0058-14.2015.

Hamood AW, Marder E. Animal-to-animal variability in neuromodulation and circuit function. *Cold Spring Harb Symp Quant Biol* 79: 21–28, 2014. [Erratum in *Cold Spring Harb Symp Quant Biol* 79: 309, 2014.] doi:10.1101/sqb.2014.79.024828.

Heinzel HG. Gastric mill activity in the lobster. I. Spontaneous modes of chewing. *J Neurophysiol* 59: 528–550, 1988. doi:10.1152/jn.1988.59.2.528.

Heinzel HG, Weimann JM, Marder E. The behavioral repertoire of the gastric mill in the crab, *Cancer pagurus*: an in situ endoscopic and electrophysiological examination. *J Neurosci* 13: 1793–1803, 1993. doi:10.1523/JNEUROSCI.13-04-01793.1993.

Hermans EJ, van Marle HJF, Ossewaarde L, Henckens MJAG, Qin S, van Kesteren MTR, Schoots VC, Cousijn H, Rijpkema M, Oostenveld R, Fernández G. Stress-related noradrenergic activity prompts large-scale neural network reconfiguration. *Science* 334: 1151–1153, 2011. doi:10.1126/science.1209603.

Hooper SL, Marder E. Modulation of the lobster pyloric rhythm by the peptide proctolin. *J Neurosci* 7: 2097–2112, 1987. doi:10.1523/JNEUROSCI.07-07-02097.1987.

Hooper SL, Moulins M. Switching of a neuron from one network to another by sensory-induced changes in membrane properties. *Science* 244: 1587–1589, 1989. doi:10.1126/science.2740903.

Hooper SL, O'Neil MB, Wagner R, Ewer J, Golowasch J, Marder E. The innervation of the pyloric region of the crab, *Cancer borealis*: homologous muscles in decapod species are differently innervated. *J Comp Physiol A Neuroethol Sens Neural Behav Physiol* 159: 227–240, 1986. doi:10.1007/BF00612305.

Huybrechts J, Nusbaum MP, Bosch LV, Baggerman G, De Loof A, Schoofs L. Neuropeptidomic analysis of the brain and thoracic ganglion from the Jonah crab, *Cancer borealis*. *Biochem Biophys Res Commun* 308: 535–544, 2003. doi:10.1016/S0006-291X(03)01426-8.

Jacobs J, Kahana MJ, Ekstrom AD, Fried I. Brain oscillations control timing of single-neuron activity in humans. *J Neurosci* 27: 3839–3844, 2007. doi:10.1523/JNEUROSCI.4636-06.2007.

Jékely G, Melzer S, Beets I, Kadow ICG, Koene J, Haddad S, Holden-Dye L. The long and the short of it - a perspective on peptidergic regulation of circuits and behaviour. *J Exp Biol* 221: jeb166710, 2018. doi:10.1242/jeb.166710.

Jiang X, Chen R, Wang J, Metzler A, Tlusty M, Li L. Mass spectral charting of neuropeptidomic expression in the stomatogastric ganglion at multiple developmental stages of the lobster *Homarus americanus*. *ACS Chem Neurosci* 3: 439–450, 2012. doi:10.1021/cn200107v.

Johnson BR, Peck JH, Harris-Warrick RM. Amine modulation of electrical coupling in the pyloric network of the lobster stomatogastric ganglion. *J Comp Physiol A Neuroethol Sens Neural Behav Physiol* 172: 715–732, 1993. doi:10.1007/BF00195397.

Katz PS. Phylogenetic plasticity in the evolution of molluscan neural circuits. *Curr Opin Neurobiol* 41: 8–16, 2016. doi:10.1016/j.conb.2016.07.004.

Kilman VL, Marder E. Ultrastructure of the stomatogastric ganglion neuropil of the crab, *Cancer borealis*. *J Comp Neurol* 374: 362–375, 1996. doi:10.1002/(SICI)1096-9861(19961021)374:3<362::AID-CNE5>3.0.CO;2-#.

Kirby MS, Nusbaum MP. Central nervous system projections to and from the commissural ganglion of the crab *Cancer borealis*. *Cell Tissue Res* 328: 625–637, 2007. doi:10.1007/s00441-007-0398-2.

Ko KI, Root CM, Lindsay SA, Zaninovich OA, Shepherd AK, Wasserman SA, Kim SM, Wang JW. Starvation promotes concerted modulation of appetitive olfactory behavior via parallel neuromodulatory circuits. *eLife* 4: e08298, 2015. doi:10.7554/eLife.08298.

Komuniecki R, Hapiak V, Harris G, Bamber B. Context-dependent modulation reconfigures interactive sensory-mediated microcircuits in *Caenorhabditis elegans*. *Curr Opin Neurobiol* 29: 17–24, 2014. doi:10.1016/j.conb.2014.04.006.

Kwiatkowski MA, Gabranski ER, Huber KE, Chapline MC, Christie AE, Dickinson PS. Coordination of distinct but interacting rhythmic motor programs by a modulatory projection neuron using different co-transmitters in different ganglia. *J Exp Biol* 216: 1827–1836, 2013. doi:10.1242/jeb.082503.

Lane BJ, Kick DR, Wilson DK, Nair SS, Schulz DJ. Dopamine maintains network synchrony via direct modulation of gap junctions in the crustacean cardiac ganglion. *eLife* 7: e39368, 2018. doi:10.7554/eLife.39368.

Larson CR, Yajima Y, Ko P. Modification in activity of medullary respiratory-related neurons for vocalization and swallowing. *J Neurophysiol* 71: 2294–2304, 1994. doi:10.1152/jn.1994.71.6.2294.

Lillvis JL, Katz PS. Parallel evolution of serotonergic neuromodulation underlies independent evolution of rhythmic motor behavior. *J Neurosci* 33: 2709–2717, 2013. doi:10.1523/JNEUROSCI.4196-12.2013.

Lismont E, Mortelmans N, Verlinden H, Vanden Broeck J. Molecular cloning and characterization of the SIFamide precursor and receptor in a hymenopteran insect, *Bombus terrestris*. *Gen Comp Endocrinol* 258: 39–52, 2018. doi:10.1016/j.ygcen.2017.10.014.

Ma M, Wang J, Chen R, Li L. Expanding the Crustacean neuropeptidome using a multifaceted mass spectrometric approach. *J Proteome Res* 8: 2426–2437, 2009. doi:10.1021/pr801047v.

Marder E. Neuromodulation of neuronal circuits: back to the future. *Neuron* 76: 1–11, 2012. doi:10.1016/j.neuron.2012.09.010.

Marder E, Bucher D. Understanding circuit dynamics using the stomatogastric nervous system of lobsters and crabs. *Annu Rev Physiol* 69: 291–316, 2007. doi:10.1146/annurev.physiol.69.031905.161516.

Marder E, Gutierrez GJ, Nusbaum MP. Complicating connectomes: electrical coupling creates parallel pathways and degenerate circuit mechanisms. *Dev Neurobiol* 77: 597–609, 2017. doi:10.1002/dneu.22410.

Marder E, Hooper SL, Siwicki KK. Modulatory action and distribution of the neuropeptide proctolin in the crustacean stomatogastric nervous system. *J Comp Neurol* 243: 454–467, 1986. doi:10.1002/cne.902430403.

Marder E, O'Leary T, Shruti S. Neuromodulation of circuits with variable parameters: single neurons and small circuits reveal principles of state-dependent and robust neuromodulation. *Annu Rev Neurosci* 37: 329–346, 2014. doi:10.1146/annurev-neuro-071013-013958.

Martelli C, Pech U, Kobbenbring S, Pauls D, Bahl B, Sommer MV, Pooryasin A, Barth J, Arias CWP, Vassiliou C, Luna AJF, Poppinga H, Richter FG, Wegener C, Fiala A, Riemensperger T. SIFamide translates hunger signals into appetitive and feeding behavior in Drosophila. *Cell Reports* 20: 464–478, 2017. doi:10.1016/j.celrep.2017.06.043.

Merighi A, Salio C, Ferrini F, Lossi L. Neuromodulatory function of neuropeptides in the normal CNS. *J Chem Neuroanat* 42: 276–287, 2011. doi:10.1016/j.jchemneu.2011.02.001.

Meyrand P, Faumont S, Simmers J, Christie AE, Nusbaum MP. Species-specific modulation of pattern-generating circuits. *Eur J Neurosci* 12: 2585–2596, 2000. doi:10.1046/j.1460-9568.2000.00121.x.

Meyrand P, Weimann JM, Marder E. Multiple axonal spike initiation zones in a motor neuron: serotonin activation. *J Neurosci* 12: 2803–2812, 1992. doi:10.1523/JNEUROSCI.12-07-02803.1992.

Miller JP, Selverston A. Rapid killing of single neurons by irradiation of intracellularly injected dye. *Science* 206: 702–704, 1979. doi:10.1126/science.386514.

Nadim F, Bucher D. Neuromodulation of neurons and synapses. *Curr Opin Neurobiol* 29: 48–56, 2014. doi:10.1016/j.conb.2014.05.003.

Nässel DR. Tachykinin-related peptides in invertebrates: a review. *Peptides* 20: 141–158, 1999. doi:10.1016/S0196-9781(98)00142-9.

Nässel DR. Neuropeptides in the nervous system of *Drosophila* and other insects: multiple roles as neuromodulators and neurohormones. *Prog Neurobiol* 68: 1–84, 2002. doi:10.1016/S0301-0082(02)00057-6.

Nässel DR. Substrates for neuronal cotransmission with neuropeptides and small molecule neurotransmitters in *Drosophila*. *Front Cell Neurosci* 12: 83, 2018. doi:10.3389/fncel.2018.00083.

Nässel DR, Wegener C. A comparative review of short and long neuropeptide F signaling in invertebrates: any similarities to vertebrate neuropeptide Y signaling? *Peptides* 32: 1335–1355, 2011. doi:10.1016/j.peptides.2011.03.013.

Norris BJ, Coleman MJ, Nusbaum MP. Pyloric motor pattern modification by a newly identified projection neuron in the crab stomatogastric nervous system. *J Neurophysiol* 75: 97–108, 1996. doi:10.1152/jn.1996.75.1.97.

Nusbaum MP, Blitz DM. Neuropeptide modulation of microcircuits. *Curr Opin Neurobiol* 22: 592–601, 2012. doi:10.1016/j.conb.2012.01.003.

Nusbaum MP, Blitz DM, Marder E. Functional consequences of neuropeptide and small-molecule co-transmission. *Nat Rev Neurosci* 18: 389–403, 2017. doi:10.1038/nrn.2017.56.

Nusbaum MP, Blitz DM, Swensen AM, Wood D, Marder E. The roles of co-transmission in neural network modulation. *Trends Neurosci* 24: 146–154, 2001. doi:10.1016/S0166-2236(00)01723-9.

Nusbaum MP, Marder E. A modulatory proctolin-containing neuron (MPN). I. Identification and characterization. *J Neurosci* 9: 1591–1599, 1989a. doi:10.1523/JNEUROSCI.09-05-01591.1989.

Nusbaum MP, Marder E. A modulatory proctolin-containing neuron (MPN). II. State-dependent modulation of rhythmic motor activity. *J Neurosci* 9: 1600–1607, 1989b. doi:10.1523/JNEUROSCI.09-05-01600.1989.

Nusbaum MP, Weimann JM, Golowasch J, Marder E. Presynaptic control of modulatory fibers by their neural network targets. *J Neurosci* 12: 2706–2714, 1992. doi:10.1523/JNEUROSCI.12-07-02706.1992.

O'Brien J. The ever-changing electrical synapse. *Curr Opin Neurobiol* 29: 64–72, 2014. doi:10.1016/j.conb.2014.05.011.

Ohno H, Yoshida M, Sato T, Kato J, Miyazato M, Kojima M, Ida T, Iino Y. Luqin-like RYamide peptides regulate food-evoked responses in *C. elegans*. *eLife* 6: e28877, 2017. doi:10.7554/eLife.28877.

Park S, Sonn JY, Oh Y, Lim C, Choe J. SIFamide and SIFamide receptor defines a novel neuropeptide signaling to promote sleep in *Drosophila. Mol Cells* 37: 295–301, 2014. doi:10.14348/molcells.2014.2371.

Pereda AE, Curti S, Hoge G, Cachope R, Flores CE, Rash JE. Gap junction-mediated electrical transmission: regulatory mechanisms and plasticity. *Biochim Biophys Acta* 1828: 134–146, 2013. [Erratum in *Biochim Biophys Acta* 1838: 1056, 2014.] doi:10.1016/j.bbamem.2012.05.026.

Polanska MA, Yasuda A, Harzsch S. Immunolocalisation of crustacean-SIFamide in the median brain and eyestalk neuropils of the marbled crayfish. *Cell Tissue Res* 330: 331–344, 2007. doi:10.1007/s00441-007-0473-8.

Qiu J, Nestor CC, Zhang C, Padilla SL, Palmiter RD, Kelly MJ, Rønnekleiv OK. High-frequency stimulation-induced peptide release synchronizes arcuate kisspeptin neurons and excites GnRH neurons. *eLife* 5: e16246, 2016. doi:10.7554/eLife.16246.

Rehm KJ, Taylor AL, Pulver SR, Marder E. Spectral analyses reveal the presence of adult-like activity in the embryonic stomatogastric motor patterns of the lobster, *Homarus americanus. J Neurophysiol* 99: 3104–3122, 2008. doi:10.1152/jn.00042.2008.

Rodriguez JC, Blitz DM, Nusbaum MP. Convergent rhythm generation from divergent cellular mechanisms. *J Neurosci* 33: 18047–18064, 2013. doi:10.1523/JNEUROSCI.3217-13.2013.

Saideman SR, Blitz DM, Nusbaum MP. Convergent motor patterns from divergent circuits. *J Neurosci* 27: 6664–6674, 2007a. doi:10.1523/JNEUROSCI.0315-07.2007.

Saideman SR, Christie AE, Torfs P, Huybrechts J, Schoofs L, Nusbaum MP. Actions of kinin peptides in the stomatogastric ganglion of the crab *Cancer borealis. J Exp Biol* 209: 3664–3676, 2006. doi:10.1242/jeb.02415.

Saideman SR, Ma M, Kutz-Naber KK, Cook A, Torfs P, Schoofs L, Li L, Nusbaum MP. Modulation of rhythmic motor activity by pyrokinin peptides. *J Neurophysiol* 97: 579–595, 2007b. doi:10.1152/jn.00772.2006.

Sakurai A, Katz PS. Artificial synaptic rewiring demonstrates that distinct neural circuit configurations underlie homologous behaviors. *Curr Biol* 27: 1721–1734.E3, 2017. doi:10.1016/j.cub.2017.05.016.

Saunders SW, Rath D, Hodges PW. Postural and respiratory activation of the trunk muscles changes with mode and speed of locomotion. *Gait Posture* 20: 280–290, 2004. doi:10.1016/j.gaitpost.2003.10.003.

Schlegel P, Texada MJ, Miroschnikow A, Schoofs A, Hückesfeld S, Peters M, Schneider-Mizell CM, Lacin H, Li F, Fetter RD, Truman JW, Cardona A, Pankratz MJ. Synaptic transmission parallels neuromodulation in a central food-intake circuit. *eLife* 5: e16799, 2016. doi:10.7554/eLife.16799.

Sellami A, Veenstra JA. SIFamide acts on fruitless neurons to modulate sexual behavior in *Drosophila melanogaster. Peptides* 74: 50–56, 2015. doi:10.1016/j.peptides.2015.10.003.

Skiebe P, Schneider H. Allatostatin peptides in the crab stomatogastric nervous system: inhibition of the pyloric motor pattern and distribution of allatostatin-like immunoreactivity. *J Exp Biol* 194: 195–208, 1994.

Spencer RM, Blitz DM. Network feedback regulates motor output across a range of modulatory neuron activity. *J Neurophysiol* 115: 3249–3263, 2016. doi:10.1152/jn.01112.2015.

Städele C, Stein W. The site of spontaneous ectopic spike initiation facilitates signal integration in a sensory neuron. *J Neurosci* 36: 6718–6731, 2016. doi:10.1523/JNEUROSCI.2753-15.2016.

Stehlik LL. Diets of the brachyuran crabs *Cancer irroratus, C. borealis*, and *Ovalipes ocellatus* in the New York Bight. *J Crustac Biol* 13: 723–735, 1993. doi:10.2307/1549103.

Stein W. Modulation of stomatogastric rhythms. *J Comp Physiol A Neuroethol Sens Neural Behav Physiol* 195: 989–1009, 2009. doi:10.1007/s00359-009-0483-y.

Stein W. Stomatogastric nervous system. In: *Oxford Research Encyclopedia of Neuroscience*, 2017. doi:10.1093/acrefore/9780190264086.013.153.

Stemmler EA, Cashman CR, Messinger DI, Gardner NP, Dickinson PS, Christie AE. High-mass-resolution direct-tissue MALDI-FTMS reveals broad conservation of three neuropeptides (APSGFLGMRamide, GYRKPPFNGSIFamide and pQDLDHVFLRFamide) across members of seven decapod crustacean infraorders. *Peptides* 28: 2104–2115, 2007. doi:10.1016/j.peptides.2007.08.019.

Steriade M, Nuñez A, Amzica F. Intracellular analysis of relations between the slow (< 1 Hz) neocortical oscillation and other sleep rhythms of the electroencephalogram. *J Neurosci* 13: 3266–3283, 1993. doi:10.1523/JNEUROSCI.13-08-03266.1993.

Szabo TM, Chen R, Goeritz ML, Maloney RT, Tang LS, Li L, Marder E. Distribution and physiological effects of B-type allatostatins (myoinhibitory peptides, MIPs) in the stomatogastric nervous system of the crab *Cancer borealis. J Comp Neurol* 519: 2658–2676, 2011. doi:10.1002/cne.22654.

Taghert PH, Nitabach MN. Peptide neuromodulation in invertebrate model systems. *Neuron* 76: 82–97, 2012. doi:10.1016/j.neuron.2012.08.035.

Terhzaz S, Rosay P, Goodwin SF, Veenstra JA. The neuropeptide SIFamide modulates sexual behavior in *Drosophila. Biochem Biophys Res Commun* 352: 305–310, 2007. doi:10.1016/j.bbrc.2006.11.030.

van den Pol AN. Neuropeptide transmission in brain circuits. *Neuron* 76: 98–115, 2012. doi:10.1016/j.neuron.2012.09.014.

Vázquez-Acevedo N, Rivera NM, Torres-González AM, Rullan-Matheu Y, Ruíz-Rodríguez EA, Sosa MA. GYRKPPFNGSIFamide (Gly SIF-amide) modulates aggression in the freshwater prawn *Macrobrachium rosenbergii. Biol Bull* 217: 313–326, 2009. doi:10.1086/BBLv217n3p313.

Verleyen P, Huybrechts J, Baggerman G, Van Lommel A, De Loof A, Schoofs L. SIFamide is a highly conserved neuropeptide: a comparative study in different insect species. *Biochem Biophys Res Commun* 320: 334–341, 2004. doi:10.1016/j.bbrc.2004.05.173.

Verleyen P, Huybrechts J, Schoofs L. SIFamide illustrates the rapid evolution in arthropod neuropeptide research. *Gen Comp Endocrinol* 162: 27–35, 2009. doi:10.1016/j.ygcen.2008.10.020.

Weimann JM, Marder E. Switching neurons are integral members of multiple oscillatory networks. *Curr Biol* 4: 896–902, 1994. doi:10.1016/S0960-9822(00)00199-8.

Weimann JM, Meyrand P, Marder E. Neurons that form multiple pattern generators: identification and multiple activity patterns of gastric/pyloric neurons in the crab stomatogastric system. *J Neurophysiol* 65: 111–122, 1991. doi:10.1152/jn.1991.65.1.111.

White RS, Nusbaum MP. The same core rhythm generator underlies different rhythmic motor patterns. *J Neurosci* 31: 11484–11494, 2011. doi:10.1523/JNEUROSCI.1885-11.2011.

Wiersma CA. On the number of nerve cells in a crustacean central nervous system. *Acta Physiol Pharmacol Neerl* 6: 135–142, 1957.

Wood DE, Stein W, Nusbaum MP. Projection neurons with shared cotransmitters elicit different motor patterns from the same neural circuit. *J Neurosci* 20: 8943–8953, 2000.

Wood DE, Manor Y, Nadim F, Nusbaum MP. Intercircuit control via rhythmic regulation of projection neuron activity. *J Neurosci* 24: 7455–7463, 2004. doi:10.1523/JNEUROSCI.1840-04.2004.

Yasuda A, Yasuda-Kamatani Y, Nozaki M, Nakajima T. Identification of GYRKPPFNGSIFamide (crustacean-SIFamide) in the crayfish *Procambarus clarkii* by topological mass spectrometry analysis. *Gen Comp Endocrinol* 135: 391–400, 2004. doi:10.1016/j.ygcen.2003.10.001.

Yasuda-Kamatani Y, Yasuda A. Characteristic expression patterns of allatostatin-like peptide, FMRFamide-related peptide, orcokinin, tachykinin-related peptide, and SIFamide in the olfactory system of crayfish *Procambarus clarkii. J Comp Neurol* 496: 135–147, 2006. doi:10.1002/cne.20903.

Zatylny-Gaudin C, Favrel P. Diversity of the RFamide peptide family in mollusks. *Front Endocrinol (Lausanne)* 5: 178, 2014. doi:10.3389/fendo.2014.00178.